

Rijksuniversiteit Groningen
Faculty of Mathematics and Natural Sciences
Zernike Institute for Advanced Materials

Carbon nanotube electronics

Master thesis by

Igor Iezhokin

August 31, 2011



university of
groningen

faculty of mathematics
and natural sciences

Group: Photophysics and OptoElectronics

Group Leader: Prof. Dr. Maria-Antonietta Loi

Supervisors: Prof. Dr. Maria-Antonietta Loi

Drs. Jia Gao

Period: September 2010 – July 2011

Abstract

Single – walled carbon nanotubes (SWNTs) are very promising candidate to replace silicon in Complementary Metal Oxide Semiconductor (CMOS) technology due to their extraordinary properties. But unfortunately nowadays all synthesis methods of carbon nanotubes growing cannot provide efficient sorting between metallic and semiconducting species. In this work, the efficient scalable method for the preparation of high purity semiconducting SWNT has been reported. This was done by using sonication and ultracentrifuge procedure of the suspension consists of SWNT CoMoCAT tubes, PFO polymer in toluene in the ratio: (1 mg, 3 mg, 10 ml). At the end 99% semiconducting enriched SWNT suspension was achieved. Bottom contact FET device was made by solution processed method with SWNT network and show ambipolar behavior with device mobility in the range of 10^{-3} - 10^{-2} cm²/Vs for both types of carriers (holes and electrons respectively) with SWNT coverage less than 1%. Also we shown in current work the effect of air exposure and annealing on the performance of the transistor.

Contents

Chapter 1 Introduction

1.1 Overview

1.2 Single-walled carbon nanotubes

1.2.1 SWNT electrical and optical properties

1.2.2 Synthesis of carbon nanotubes

1.2.3 Sorting of SWNTs species.

1.3 Field Effect Transistor

1.3.1 Carbon Nanotube Ambipolar FETs

1.3.2 Carrier trapping mechanism in Carbon Nanotube Transistor

Chapter 2 Experimental

2.1 Materials and fabrication

2.1.1 PFO

2.1.2 Commercial available SWNT solution (IsoNanotubes-S)

2.1.3 CoMoCAT carbon nanotubes (SWeNT)

2.2 Preparation of the carbon PFO-SWNT solution

2.3 Optical Characterization

2.4 The substrate

2.5 Device Fabrication

2.6 I-V characteristics measurements

2.7 Microscopy

Chapter 3 Results and Discussion

3.1. SWNT suspension

3.1.1 Commercial available SWNT suspension

3.1.2 PFO and CoMoCAT mixture

3.2 Device Performance

3.2.1 Device based on commercial available solution

3.2.2 Device based on “home made” solution

- 3.2.3 Vacuum measurements
- 3.2.4 Mobility and on/off ratio calculation
- 3.2.5. Microscopy characterizations
- 3.2.6. Effective mobility calculation
- 3.2.7. Ambient effect
- 3.2.8. High-temperature annealing in air
- Chapter 4. Conclusion and future research
 - 4.1 Conclusion
 - 4.2 Future research
- Acknowledgements
- Bibliography
- Appendix A

Chapter 1

Introduction

In this chapter, first of all I will discuss the general photophysical and electrical properties of single-walled carbon nanotubes. I will also demonstrate the recent progress of the separation of semiconducting SWNTs species with metallic ones and the application of SWNTs in solid-state electronic devices. Upon giving a brief introduction into the carbon nanotube electronics, the operating principle of field effect transistor (FET) is presented. An overview recent progress on carbon nanotube transistor will be discussed. Finally, the motivation and the goals of the project will be mentioned.

1.1 Overview

The last few decades a dramatic increase in nanotechnology research progress has been achieved. Among others, one of the most exciting fields to emerge is nanoelectronics, where a myriad of possibilities are appearing in the form of sensors, actuators, and transistors, each characterized by feature sizes of the order of a few nanometres. All this innovation have been fueled by the discovery of new materials and the invention of manufacturing methods that allow design and development at such a minute scale. Carbon nanotubes are at the forefront of these new materials, due to the unique mechanical and electronic properties that give them, for example, exceptional strength and conductivity. One exciting possibility is the creation of nanometer-scale transistors, perhaps to be embedded, in the future, inside complex and miniscule electronic circuits that will make today's chips seem enormous in comparison. Moreover, these nanotubes exhibit a tremendous current-carrying ability, potentially allowing for increased miniaturization of high-speed and high-power circuits. Although some devices have already been produced, the technology is still in its infancy when compared to, for instance, that of bulk-silicon metal–oxide–semiconductor field-effect transistor (MOSFET). Since the discovery of carbon nanotubes (CNTs) by Iijima in 1991 [1], significant progress has been achieved for both understanding the fundamental properties and exploring possible engineering applications [2]. The possible application for nanoelectronic devices has been extensively explored since the demonstration of the first carbon nanotube transistors (CNTFETs) [3]. Carbon nanotubes are attractive for nanoelectronic applications due to its excellent electric properties. In a nanotube, low bias transport can be nearly ballistic across distances of several hundred nanometers. The conduction and valence bands are symmetric, which is advantageous for complementary applications. The bandstructure is direct, which enables optical emission, and finally, SWNTs are highly resistant to electromigration. Significant efforts have devoted to understand how a carbon nanotube transistor operates and to improve the transistor performance. The protocol for device fabrication could be generally described in two categories. In the first case, SWNTs are grown on a substrate by chemical vapor deposition (CVD) method at high temperature (~ 900 °C), the active components of the device can be either single tube or SWNT network [4,5]. In this project, we developed a scalable method for the preparation of high purity semiconducting SWNT dispersion that only consists of sonication and ultracentrifugation procedures. Solution processed FETs with randomly distributed SWNT network as channel show ambipolar behavior with comparable electron and holes mobilities. We also investigated the electrical characteristics of ambipolar FETs by changing the environmental conditions. On the contrary, electron transport is suppressed with exposure to air and no electron transport was observed after 1 day in air ambience. An almost recovery of the mobility for hole was obtained by re-annealing in vacuum. Annealing in air converted ambipolar SWNT devices into unipolar also increased the gate hysteresis.

1.2 Single-walled carbon nanotubes

Nanotubes are members of the fullerene structural family, which also includes the spherical bucky-balls that were discovered by Smalley and coworkers at Rice University (Kroto et al. 1985). Obviously that their name is derived from their size, since the diameter of a nanotube is on the order of few nanometers. Carbon nanotubes are hollow cylinders of carbon and were first discovered by Sumo Iijima in 1991. The structure of a carbon nanotube is typically discussed in terms of graphene, which is a single layer of sp^2 -bonded carbon atoms in a honeycomb lattice. Particularly, a SWNT can be made by rolling up graphene to form a seamless cylinder. Carbon nanotubes with one wall are called a single-walled carbon nanotubes (SWNT). If a carbon nanotube has two walls it is called a dual - walled carbon nanotube (DWNT) and in case if nanotubes have more than two walls they are called multi-walled carbon nanotubes (MWNT). The diameter of a SWNT typically ranges between 0.5 nm and 2 nm and its length can vary in range (from 10 nm to 1 cm). Like other nanomaterials, the properties of SWNTs depend on their size and atomic structure. The length can be important for some applications, but it is well known fact that SWNT properties strongly depend on their diameter and orientation of the carbon hexagons (helicity) that form their walls and this is particularly true for the electronic properties of a SWNT. The resulting diverse and exemplary properties of SWNTs could have plenty of applications including transistors, logic gates, interconnects, conductive films, field emission sources, infrared emitters, sensors, scanning probes, et.c.

A SWNT can be described as had it been created by folding a sheet of graphene. So direction in which the graphene was rolled up to form the nanotube is very important and this direction is called the chiral vector in other words - Chirality is the way of rolling graphene into a tube and is defined by a circumferential vector.

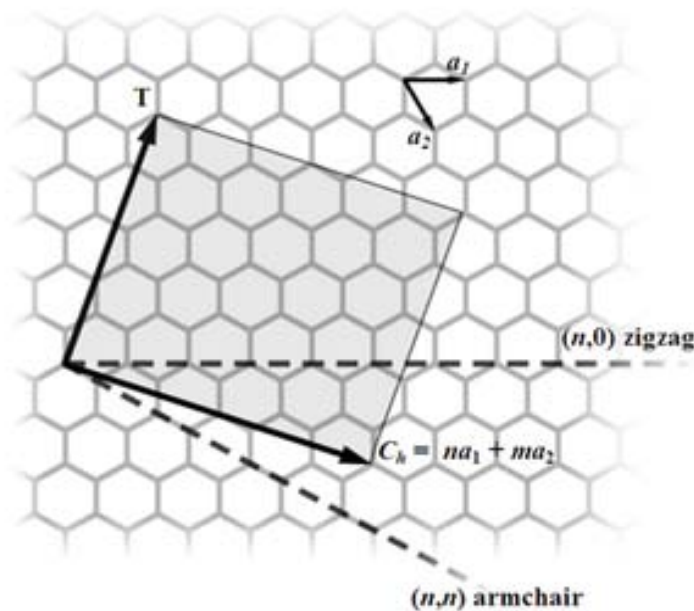


Figure 1.1 The circumference of the SWNT is determined by its chiral vector $C_h = na_1 + ma_2$, where (n,m) are integers known as the chiral indices and a_1 and a_2 are the unit vectors of the graphene lattice.

Each carbon atom in graphene can be identified with a pair of integers (n,m) and a pair of lattice vectors (a_1, a_2) , leading to the definition of the chiral vector, $\text{Ch} = na_1 + ma_2$, also diameter of the nanotube could be defined by magnitude of the chiral vector $d = \text{Ch}/\pi$. The formation of a chiral vector is further described in Figure 1.1. Also Graphene has a six fold rotational symmetry, if one combines this with mirror symmetry it is possible to describe all single nanotube using chiral vectors between 0° and 30° degrees. Carbon nanotubes with a chiral vector of 30° degrees and a equal vector numbers $(n=m)$, are an arm chair circumference and called armchair carbon nanotubes

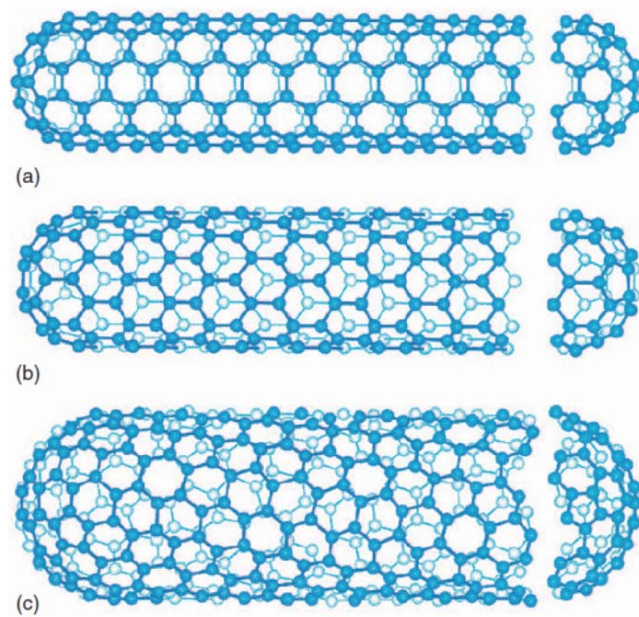


Figure1.3. Chirality of SWNTs a) Arm-chair b) Zig-zag c) Chiral

In case when carbon nanotube have a chiral vector of 0° degrees and have vector numbers of $(n,m)=(n,0)$ or $(0,m)$ then it is a zig zag circumference (zig zag nanotubes). The rest of SWNTs are called chiral nanotubes. All three kinds of nanotubes depicted in Figure 1.3.

1.2.1 Electrical and Optical Properties of SWNTs

Generally after synthesis, approximately 67% of SWNTs are semiconducting and 33% of SWNTs are metallic. As was mentioned above if n and m are equal, we have then arm chair circumference. All armchair SWNTs are metallic whereas SWNTs with $n-m=3i$ (i being an integer different than 0) are semi-metallic and $n-m \neq 3i$ are semiconducting. If $(n,m)=(n,0)$ or $(0,m)$ then it is a zig zag nanotubes and this type of nanotubes can be either metallic or semiconducting (Fig.1.3)

Optical properties of carbon nanotubes derive from electronic transitions within one-dimensional density of states (DOS). A typical feature of one-dimensional crystals is that their DOS is not a continuous function of energy, but it descends gradually and then increases in a discontinuous spike. In contrast, three-dimensional materials have continuous DOS. The sharp peaks found in one-dimensional materials are called Van Hove singularities. Van Hove singularities result in the following remarkable optical properties of carbon nanotubes.

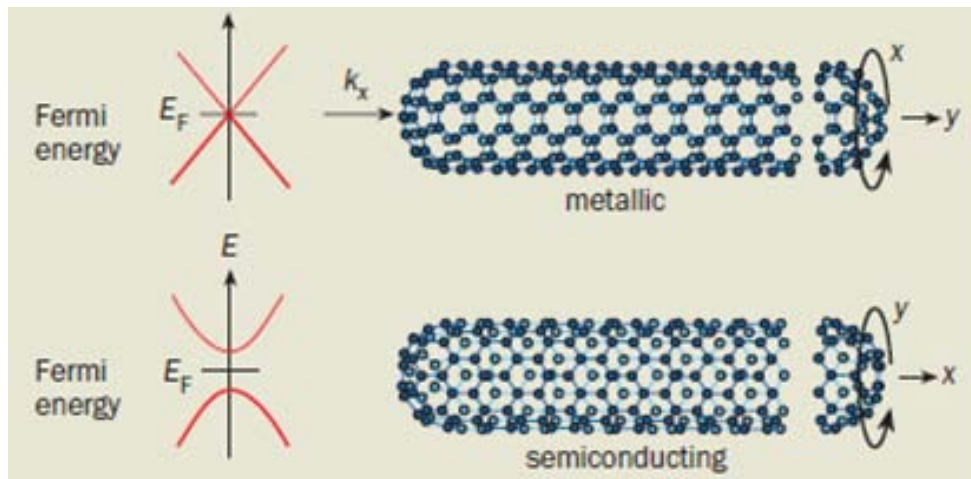


Figure 1.3. If the graphene is rolled up around the y axis, the nanotube is a metal, but if it is rolled up around the x axis, the nanotube is a semiconductor .

Optical transitions occur between the $v_1 - c_1$, $v_2 - c_2$, etc., states of semiconducting or metallic nanotubes and are traditionally labeled as S_{11} , S_{22} , M_{11} , etc., or, if the "conductivity" of the tube is unknown or unimportant, as E_{11} , E_{22} , etc. Crossover transitions $c_1 - v_2$, $c_2 - v_1$, etc., are dipole-forbidden and thus are extremely weak, but they were possibly observed using cross-polarized optical geometry. The energies between the Van Hove singularities depend on the nanotube structure. Thus by varying this structure, one can tune the optoelectronic properties of carbon nanotube.

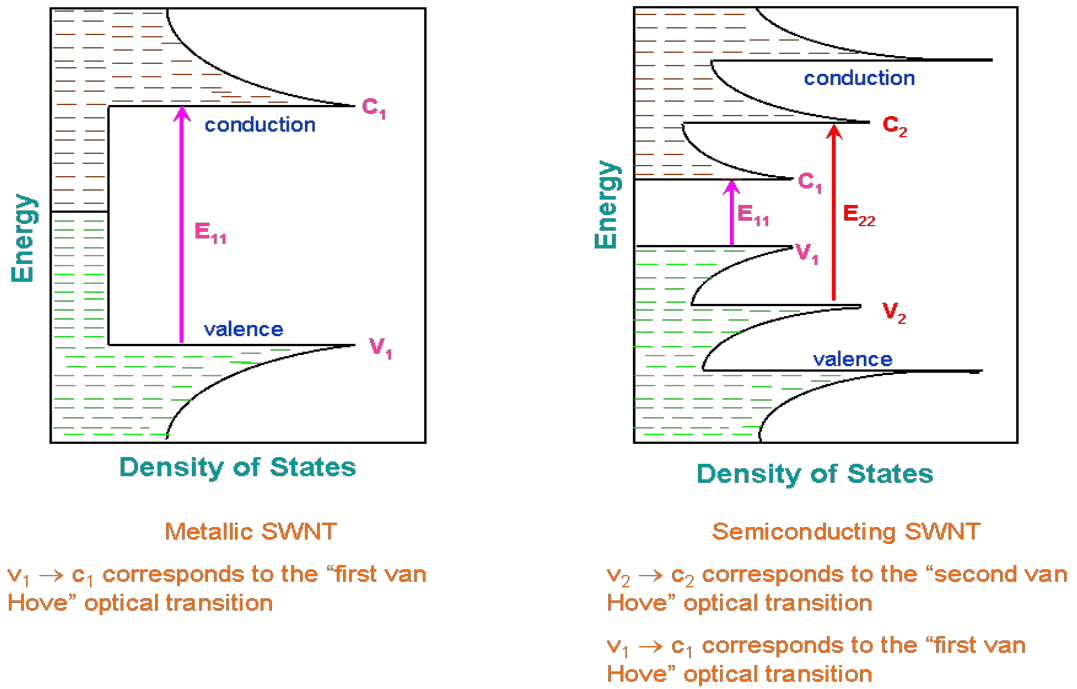


Fig.1. 4. Density of Electronic States (DOS) for a Single SWNT Structure.

Consequently, it is relatively easy to selectively excite nanotubes having certain (n, m) indices, as well as to detect optical signals from individual nanotubes. For small diameter SWNTs ($\approx 0,7-1,2$ nm) which was used in this work the E_{11} transition is typically in the range 900 to 1500 nm, for the E_{22} transition this range is 600 to 900 nm. The ration E_{22} / E_{11} is generally around 1.7. For the transition wavelengths one must take into account the used solvent because different solvents have different dielectric constants, which leads to a shift in the (n,m) - specific wavelength. Due to the strong Van der Waal forces SWNTs have tendency to form bundles. In terms to achieve uniform electrical and optical properties, SWNTs need to be monodisperse . Sonication procedure is one of the technique that allows us to broke bundles. So to achieve optimal performance in all conceivable applications, SWNTs species should be monodisperse with respect to electronic type, diameter, length and chiral handedness. Experimental methods for determining the degree of monodispersity include microscopy (for example, atomic force microscopy, scanning tunneling microscopy and electron microscopy), optical spectroscopy (for example, optical absorbance, photoluminescence and Raman spectroscopy), and charge transport measurements.

1.2.2 Synthesis of carbon nanotubes

Due to the fact that SWNTs are thermodynamically stable forms of carbon that are produced when a carbonaceous feedstock is exposed to a metal catalyst at high temperatures, there are several ways of SWNTs synthesis, include: (1) arc discharge [6], where a plasma is struck between graphite rods; (2) laser ablation [7], where a high-intensity laser beam is focused on a graphite rod; (3) chemical vapor deposition [8], where a carbon-bearing gas is heated in a furnace. Some progress of controlling the properties of SWNTs during growth procedure has

been made already. Unfortunately none of these synthetic techniques produce identical populations of SWNTs it means that final product contains both types of SWNTs species, metallic and semiconducting one. This fact leads to the primary reasons why SWNTs are rarely used in commercial applications today. Particularly in this work was used product that was grown by unique synthesis method CoMoCAT. The strategy used in the CoMoCAT method is to keep the active Cobalt species (Co) stabilized in a non-metallic state by interaction with Molybdenum oxide (MoO_3) before it is reduced by the carbon-containing compound (CO). When exposed to carbon monoxide, the Co-Mo dual oxide is carburized, producing Molybdenum carbide and small metallic Co clusters, which remain in a high state of dispersion and result in high selectivity towards SWNT of very small diameter. As was mentioned above optical absorption can be used to evaluate the distribution of (n,m) species in a given sample. Typical spectrum corresponds to a sample obtained at 850°C by the Co-Mo catalyst is shown in the picture below (Fig.1.5). One can see a broader range of diameters (0.75-1.22 nm) and chiral angles (19-30 degrees). From absorption spectrum is possible to see that in this sample, we can see both types of species metallic and semiconducting. If we compare for instance one as clear to see metallic/semiconducting type ratio is close to the statistical ratio, near 0.5. This is good example why it is not possible to use SWNTs product in transistor application immediately after synthesis.

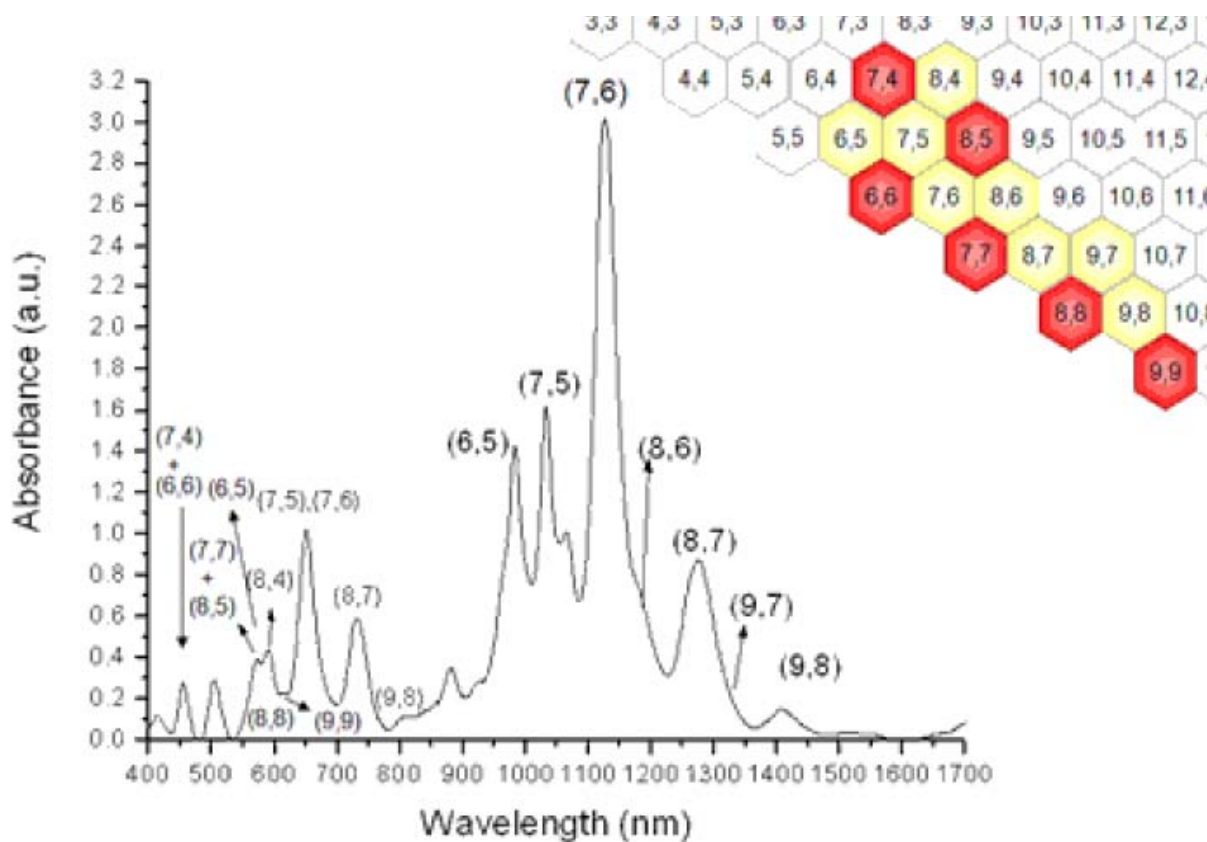


Fig.1.5 Optical absorption spectra showing a wider geometric range of nanotube CoMoCAT materials. Semiconducting species is shown as yellow hexagons and metallic as red ones.

1.2.3 Sorting of SWNTs species.

In terms to overcome this problem of separation of SWNT species, researchers have invested substantial effort towards the development of post-synthetic sorting schemes and selective growth methods for the production of bulk samples of monodisperse SWNTs [9,10].

However, beyond achieving the highest possible purity, an effective SWNT sorting strategy should also be: scalable; compatible with the wide range of SWNT lengths and diameters that are present in as-synthesized SWNT material; nondestructive (properties of SWNTs should not be degraded during sorting); iteratively repeatable (that is, it should be possible to repeat the sorting process to achieve improved purity levels); affordable, thus enabling economical incorporation into target applications. Ultimately, a SWNT sorting strategy can be deemed to have successfully met these additional criteria once its resulting material has found wide spread use in commercial applications. The key challenge for nanocomposite materials is to obtain a homogenous dispersion of nanotubes. Because of their small size, the attractive Van der Waals interactions between nanotubes are very strong and this strong interaction causes agglomeration of SWNTs. Especially, SWNTs aggregate to form bundles that are very difficult to disperse and these bundles are entangled with one another. Sonication is a simple technique that uses high-intensity acoustic energy to mix and disperse materials. During sonication, nanotube entanglements are reduced. However, this technique damages and degrades the structure of the fillers which in turn could eventually reduce the length of the nanotubes. There are several methods, materials and techniques that are used in selective sorting of SWNTs. The most popular are density gradient ultracentrifugation, chromatography, gel electrophoresis and polymer wrapping. Many different ionic surfactants as SDBS, SDS, DDBS [11,12,13] have been used before but these materials have interaction with all species in the solution. So for effective selective procedure of sorting SWNTs by diameter density gradient technique is needed.

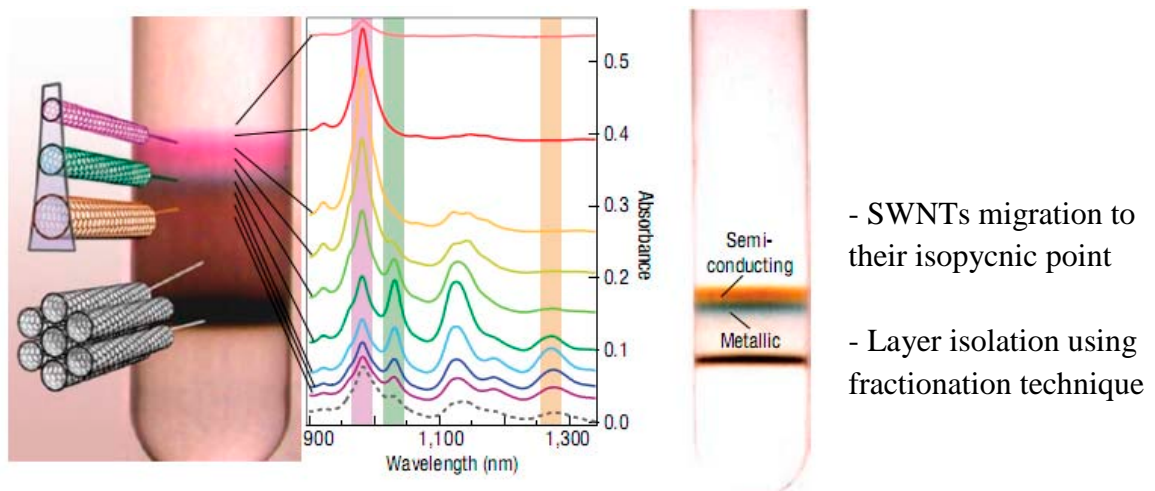


Fig. 1.6. Scheme of density gradient ultracentrifugation . Different color layers correspond to the different sorted SWNTs obtained by applying density gradient ultracentrifugation [14].

At the scheme Fig.6 density gradient ultracentrifuge procedure is shown. Generally this technique usually use for isolated and purifying cells, viruses etc. in life science. Aslo

ultracentrifugation technique could be applied for the SWNTs purpose. Especially, it is necessary to underline about the importance of conjugated polymers. A conjugated polymer can bind to a SWNT through π - π stacking, which is non-covalent interaction. As SWNT is a rolled up graphen sheet the π -orbitals are orthogonal to the surface. A π -conjugated polymer can bind to the SWNT by overlapping the π -orbitals, concerning fact that this process is opposite to a covalent bond so in this way no electrons are shared non-covalent bonds are weaker than covalent bonds, but a large amount of these bonds are formed π - π stacking and in this way is able to bind a polymer to SWNT (Fig.1.7). Recently (Ploy[9,9-dioctylfluorenyl-2,7-diy])PFO polymer has been reported [15] to selectively sort SWNTs in toluene and later several combinations of polyfluorene-based polymers and solvents were reported to give different selectivities [16,17]. In these reports become clear that slight changes to the backbone or the sidegroup of the polymer drastically changes the selectivity towards certain SWNT species, also it was reported that the different selectivities are largely depend on different conformations of the polymer in the solvent. For instance if the polymer has a low solubility in the solvent it will tend to avoid the solvent molecules and will fold. Generally it can be said that the more conformations are possible for the polymer, the lower selectivity will be. In current work we have chosen combination PFO/Toluene which shows a remarkable selectivity towards CoMoCAT product species (7,5), (7,6),(8,6),(8,7) and (9,7), which are all semiconducting.



Fig.1. 7. Schematic drawing for the molecular design of copolymers that induce SWNT chirality recognition/extraction.

In order to extract the preferred SWNTs as much as possible, all the variables including sonication and centrifugation should be optimized.

1.3. Field Effect Transistor.

A field-effect transistor (organic or inorganic) requires the following components (shown in Figure 2a): a thin semiconducting layer, which is separated from a gate electrode by the insulating gate dielectric; source and drain electrodes of width W (channel width) separated by a distance L (channel length) that are in contact with the semiconducting layer. The semiconducting layer in the case of an organic FET is usually vacuum sublimed, spin-coated, or drop-cast depending on the semiconductor. The gate electrode can be a metal or a conducting polymer, but very often, highly doped silicon serves as substrate and gate electrode at once.

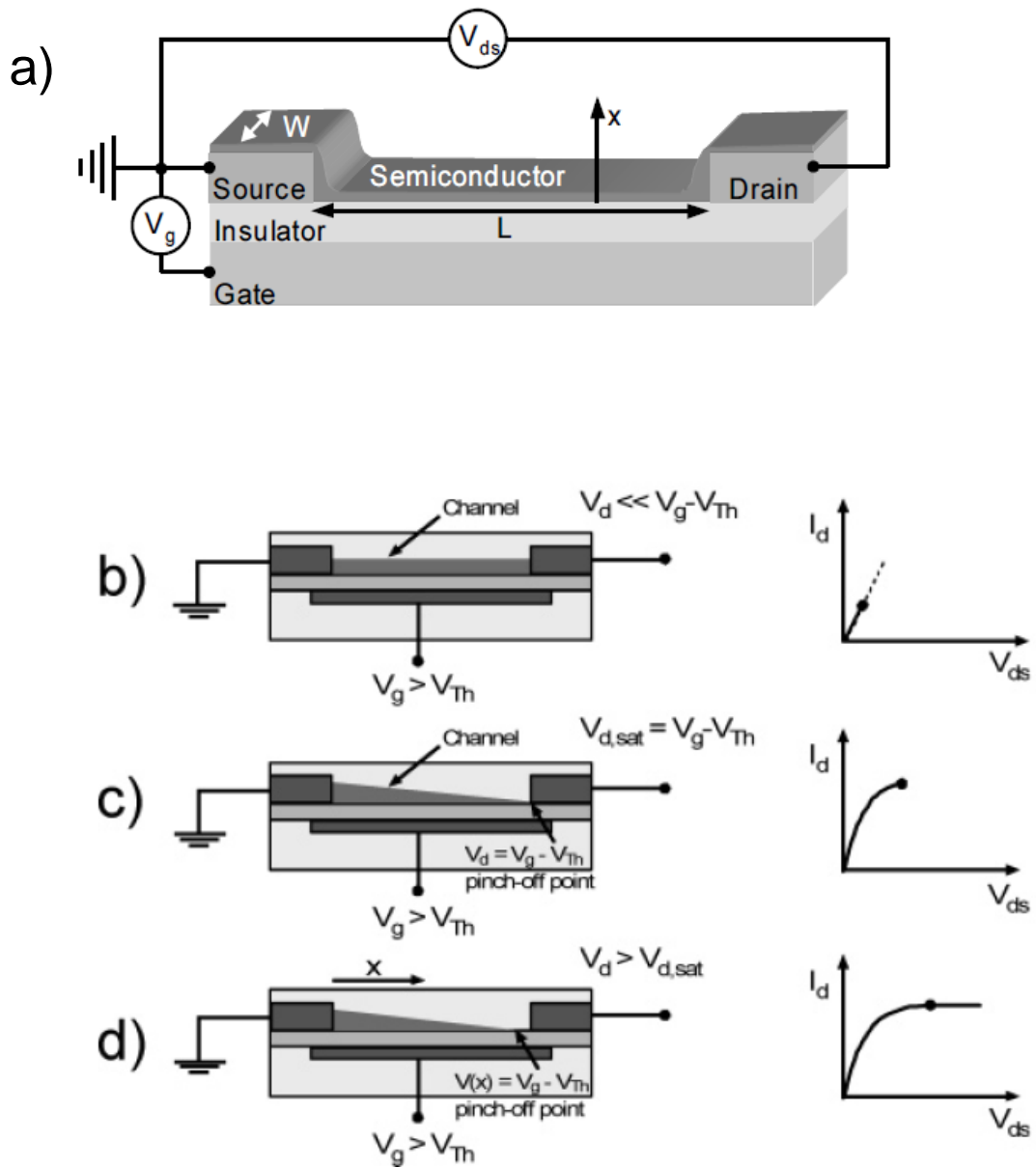


Figure 1.8. (a) Schematic structure of a field-effect transistor and applied voltages: L -channel length; W - channel width; V_d -drain voltage; V_g -gate voltage; V_{Th} - threshold voltage; I_d - drain current. (b-d) Illustrations of operating regimes of field-effect transistors: (b) linear regime; (c) start of saturation regime at pinchoff; (d) saturation regime and corresponding current-voltage characteristics.

As gate dielectrics, inorganic insulators, such as, for example, SiO_2 (thermally grown on Si or sputtered), Al_2O_3 , and Si_3N_4 , or polymeric insulators, such as poly(methyl methacrylate) (PMMA) or poly(4-vinylphenol) (PVP) are commonly used depending on the transistor structure. The source and drain electrodes, which inject charges into the semiconductor, are usually high work function metals such as gold, but conducting polymers which can be printed, are used as well.

Voltage is usually applied to the gate electrode (V_g) and the drain electrode (V_d). The source electrode is normally grounded ($V_s = 0$). The potential difference between the source and the gate is usually just called the gate voltage (V_g), while the potential difference between the source and the drain is referred to as the source-drain voltage (V_{ds}). The source is the charge-injecting electrode, as it is always more negative than the gate electrode when a positive gate voltage is applied (electrons are injected) and more positive than the gate electrode when a negative gate voltage is applied (holes are injected). Figure 1.8(b-d) illustrates the basic operating regimes of a field-effect transistor. A positive gate voltage for example will induce negative charges (electrons) at the insulator/semiconductor interface that were injected from the grounded electrodes. For negative V_g , positive charges (holes) will be accumulated. The number of accumulated charges is proportional to V_g and the capacitance C_i of the insulator. However, not all induced charges are mobile and will thus contribute to the current in a field-effect transistor. Deep traps first have to be filled before the additionally induced charges can be mobile. That is, a gate voltage has to be applied that is higher than a threshold voltage V_{Th} , and thus, the effective gate voltage is $V_g - V_{Th}$. On the other hand, donor (for n-channel) or acceptor (for p-channel) states and interface dipoles can create an internal potential at the interface and thus cause accumulation of charges in the channel when $V_g = 0$ so that in some cases an opposite voltage has to be applied to turn the channel off. When no source-drain bias is applied, the charge carrier concentration in the transistor channel is uniform. A linear gradient of charge density from the carrier injecting source to the extracting drain forms when a small source-drain voltage is applied (V_{ds} , V_g , Figure 1.8 (b)). This is the linear regime, in which the current flowing through the channel is directly proportional to V_{ds} . The potential $V(x)$ within the channel increases linearly from the source ($x=0$, $V(x) = 0$) to V_{ds} at the drain electrode ($x = L$, $V(x) = V_{ds}$). When the source-drain voltage is further increased, a point $V_{ds} = V_g - V_{Th}$ is reached, at which the channel is “pinched off” (Figure 1.8 (c)). That means a depletion region forms next to the drain because the difference between the local potential $V(x)$ and the gate voltage is now below the threshold voltage. A space-charge-limited saturation current $I_{ds,sat}$ can flow across this narrow depletion zone as carriers are swept from the pinch-off point to the drain by the comparatively high electric field in the depletion region. Further increasing the source-drain voltage will not substantially increase the current but leads to an expansion of the depletion region and thus a slight shortening of the channel. Since the potential at the pinch-off point remains $V_g - V_{Th}$ and thus the potential drop between that point and the source electrode stays approximately the same, the current saturates at a level $I_{ds,sat}$ (Figure 1.8 (d)). In this work a SWNT transistor based on solution processed method is realized and current-voltage characteristics of it in the different operating regimes could be described in approach of gradual channel approximation. It means, that the field perpendicular to the current flow generated by the gate voltage is much larger than the electric field parallel to the current flow created by the drain voltage. This is valid for long channel transistors but starts to fail for very short channel lengths. Concerning well known fact that for individual carbon nanotube the mobility described ballistically [18] and also that transistor in our case build from many carbon nanotubes mixed with residue of other carbon structures and PFO, so our percolation channel is relatively long, and we can easily use approach discussed above. So form our capacitor model of FET we have two distinct mobilities: the linear mobility in the linear regime and saturated mobility in the saturation regime:

$$\mu_{linear} = \frac{L}{WC_i V_{DS}} \left(\frac{\partial I_{DS}}{\partial V_g} \right)_{V_{DS} \rightarrow 0} \text{ (linear regime) } \quad (1.1)$$

$$\mu_{saturation} = \frac{L}{2WC_i I_{D,Sat}} \left(\frac{\partial I_{D,Sat}}{\partial V_g} \right)^2 \text{ (saturated regime) } \quad (1.2)$$

Where μ represents the mobility in either the linear or saturated regime, L is the length of the channel, W represents the width of the channel C_i the capacitance of the dielectric, I_{DS} is the current from the source to drain, $I_{D,Sat}$ equals the current from the source to the drain in the saturated regime and V_g is the gate voltage. The dielectric of the transistor described in the report is silicon oxide SiO_2 , which has dielectric constant of 3.9.

Another important parameter of FETs that can be extracted from the transfer characteristics is the on/off ratio, which is the ratio of the drain current in the on-state at a particular gate voltage and the drain current in the off-state (I_{on}/I_{off}). For clean switching behavior of the transistor, this value should be as large as possible. In situations where contact resistance effects at the source-drain electrodes can be neglected, the on-current mainly depends on the mobility of the semiconductor and the capacitance of the gate dielectric. The magnitude of the off-current is determined by gate leakage, especially for unpatterned gate electrodes and semiconductor layers, by the conduction pathways at the substrate interface, and by the bulk conductivity of the semiconductor, which can increase due to unintentional doping

1.3.1 Carbon Nanotube Field Effect Transistor

It has been demonstrated that most CNTFETs to date operates like non-conventional Schottky barrier transistors [19,20], which results in quite different device and scaling behaviors from the MOSFET-like transistors [21,22]. Also it is necessary to say about important techniques for significantly improving of the transistor performance, including the aggressively scaling of the nanotube channel and integration of thin gate dielectric insulator [23]. Another approach is solution processed methods which means that SWNT powder are firstly dispersed in aqueous or organic solution and then the dispersion could be deposited on the substrate with pre-pattered electrodes by spincoating or dropcasting method. The second process scheme allows for large area device preparation and low temperature process which are certainly more suitable for further device integration. However, the transport of electrons is strongly suppressed or completely absent in the device fabricated[24,25,26]. The origin of the suppression of electron transport is still unclear. One of the generally held views is that electron injection is obstructed due to the Schottky barriers at metal/SWNTs interface[27] Recently, Martel et al. demonstrate that the oxygen/water couple could suppress electron conduction in SWNTs much like in organic semiconductors[28].

As we mentioned before carbon nanotubes are quasi-one-dimensional objects with unique electronic properties and are attracting increasing attention due to their interesting physics and potential application in electronics and sensing. Field-effect transistors based on single semiconducting single-walled carbon nanotubes (s-SWNTs) [29] can be tuned to be p-type, n-type, or ambipolar by using appropriate injecting electrodes or doping. Vacuum-annealed SWNT-FETs with titanium electrodes show ambipolar characteristics due to thin Schottky barriers at the source and drain contacts that allow thermally assisted tunneling of holes and electrons into the nanotube and thus ambipolar transport [30]. When the gate is biased in between the source and the drain potential, polarized infrared light is emitted from the nanotube due to the radiative recombination of injected holes and electrons[31]. The wavelength of emission depends on the diameter and thus the direct band gap of the carbon nanotube. Freitag et al. showed that the location of recombination and emission is controlled by the gate voltage and can be resolved in long ($100 \mu\text{m}$) SWNT transistors. During a constant current scan, the emission zone moves with changing gate voltage from the drain to the source and vice versa [32].

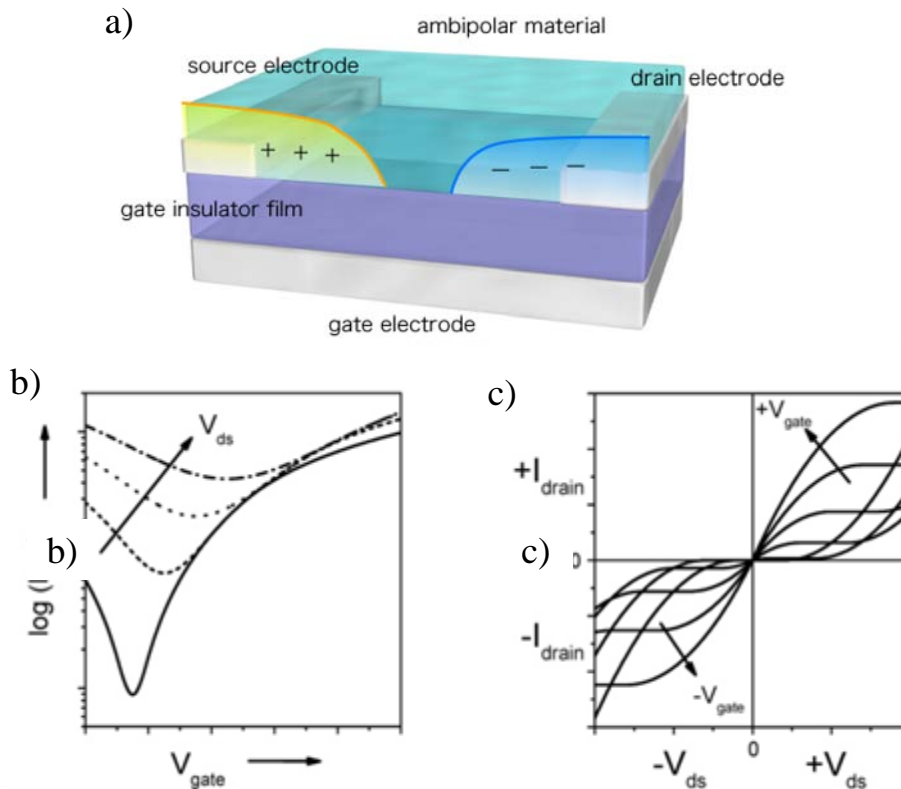


Figure 1.9. a) Schematic illustration of ambipolar field-effect transistor. b) Calculated transfer characteristics for an ambipolar transistor with equal hole and electron mobilities c) Calculated ambipolar output characteristics for the same transistor for positive and negative V_g and V_{ds} , voltages respectively.

Generally speaking typical output characteristics of a field-effect transistor demonstrate operation both in the hole-enhancement and electron enhancement mode. For high negative gate voltages, V_g , the transistor is in the hole enhancement mode and its performance is

identical to a unipolar transistor. At positive V_g , the transistor operates in the electron-enhancement mode and generally in case of carbon nanotubes electron mobility magnitude lower the hole mobility in hole enhancement mode. Schematic picture of the ambipolar transistor is depicted in Fig.1.9.

1.3.2 Carrier trapping mechanism in Carbon Nanotube Transistor

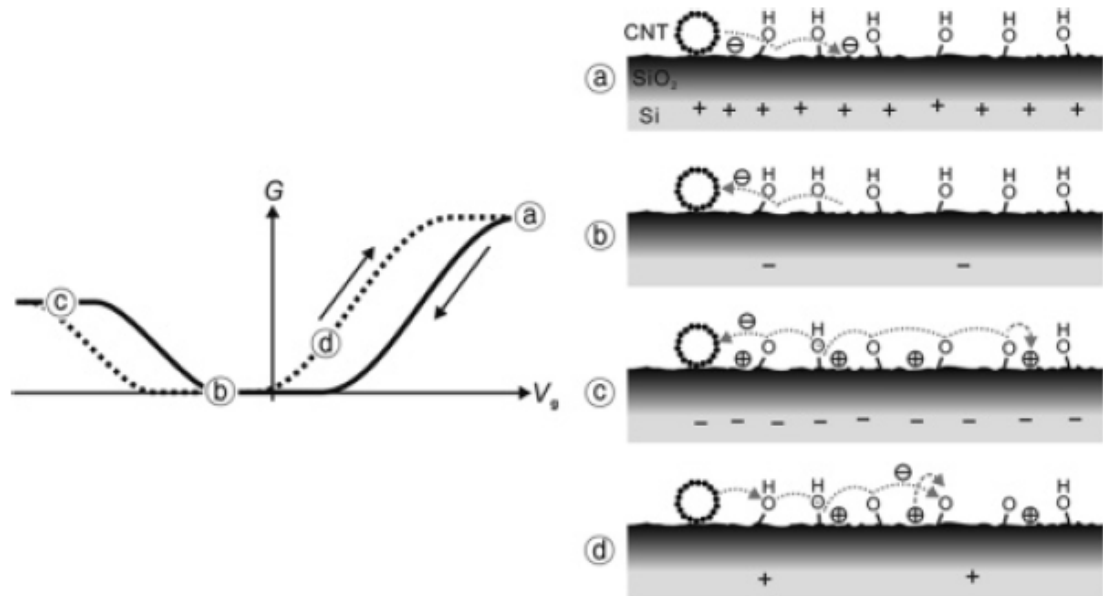


Figure. 2 Schematic of the hysteretic surface charging process in carbon nanotube FET, involving silanol groups. On the right side the trapping mechanism of the electrons is shown:

(a) at the start of a gate sweep with a positive V_g , (b) at a negative V_g in the decreasing sweep, (c) near the negative end of the decreasing sweep, and (d) at a positive V_g in the subsequent increasing sweep. The circled plus marks represent protons released from surface silanol groups. [33]

In carbon nanotube network transistor carrier injection in the oxide layer is one of the causes of carrier trapping. Other possible case is water, ions in the water layer and temperature. Temperature has no special influence on the hysteresis of SWNT FETs. Temperature does influence of the shape and size of the hysteresis, but this is only due to the influence on the available charge carriers, otherwise temperature has no effect [34]. The possibility of ions in a water layer was ruled out, because a motion of positive ions in the electric field is toward the channel for positive V_G this will create a negative shift in the gate voltage, but a positive shift is observed. [35]. Furthermore, if moving ions are the cause of the hysteresis, than hysteresis should cease to exist below a certain temperature threshold, this was not the cases. Although ions are not the cause, it has been shown that the presence of water causes hysteresis in the transfer curve. It was shown that the hysteresis in the transfer curve was higher in ambient air

than in dry air, ruling out oxygen as a cause for hysteresis. Even in after 90 hours in vacuum hysteresis was still observed. Only nanotubes which undergo extensive heat treatment and are then measured in vacuum show a drastically reduced hysteresis. Water however cannot be a trap in itself this was shown by modeling of the energy bands of carbon nanotubes and carbon nanotubes with water molecules in the vicinity. Furthermore, the hysteresis does not disappear if the sample undergoes heat treatment of up to 300 °C. The hysteresis does disappear when a monolayer of water on the surface is treated with NH₃ gas, while gas in itself has no effect. All these findings lead to the following model. Bulk charge traps are not the cause for the hysteresis. Silanol groups on the silicon oxide surface (SiOH) are the main source of trapping in carbon nanotube network transistors. A schematic of the gate-screening process involving surface silanol groups is given in Fig. 2. In this model, silanol groups may lose their protons and electrons when negative voltage V_g is applied. While the released protons are trapped nearby, the electrons are transferred into conductors (CNT or electrodes) via field driven hopping. This field-driven lateral charge hopping (or charge diffusion) should be similar to the “wetting of the surface by injected charges” observed in a contact electrification study on Al₂O₃ surfaces. The trapped net positive charges add to the gate potential, causing a negative shift of the G- V_g curve as drawn by the dotted curve in Fig. 2a. This model could explain not only gate hysteresis without surface water at low temperatures but also helps in understanding the role of surface water in gate hysteresis. At low temperatures water does not contribute to the trapping mechanism because of the immobility of the protons. At room temperature the silanol groups can be ionized, creating H₃O⁺. In this way water works as a charge trap, but only because the charge is mediated by the silanol groups. In Fig 2 (a-d) a gate sweep of carbon nanotube FET is depicted. At high positive V_G electrons from the SWNTs are trapped by the silanol SiOH groups. These electrons are reabsorbed, when V_G first becomes negative. At high negative V_G electrons from the hydrogen atoms of the surface are pulled towards the SWNT, leaving positive charges on the surface, which partially block the negative voltage of the gate. When V_G becomes positive again, these charges on the surface increase the current through the carbon nanotube. It has been proposed that silanol groups on the silicon oxide surface ($\equiv\text{SiOH}$) are the charge traps or sources subject to the deactivation. On ionization of silanol groups, the released protons can be subsequently soaked into the water layer, forming H₃O⁺; or the water layer may promote ionization of the silanol groups. The water layer here works as a proton absorbent with an intrinsic charge-screening capability. It actually works as a charge trap, but the corresponding charge transfer is mediated by the intrinsic surface charge sources, the silanol groups. In this way, humidity may influence the magnitude of hysteresis.

Chapter 2

Experimental part

2.1 Materials and fabrication

2.1.1 PFO

In order to realize the sorting procedure of semiconducting SWNT species from other product we chosen Poly[9,9-dioctylfluorenyl-2,7-diyl] (see Fig.2.1(a) also known as PFO) as dispersant and its chemical structure and some physical properties are given below. Generally speaking originally this conjugated polymer well known as light-emitting polymer. One of the main feature of PFO that it exhibits blue photo- and electroluminescence. At the Fig.2.1(b) absorption and photoluminescence measurements show that PFO has absorption peak near 378 nm and exhibits two photoluminescence peaks near 420 nm and 450 nm. PFO could be dissolved in several organic solvent such as: THF, chloroform, toluene, xylene etc. But considering the fact that during theoretical and practical studies was shown that PFO molecule has the ability to wrap around specific types of SWNTs, particularly semiconducting ones, that's why this fact can be easily used for the sorting procedure of the different species in SWNT product. In the current work it was used for the sorting of semiconducting species procedure in CoMoCAT product.

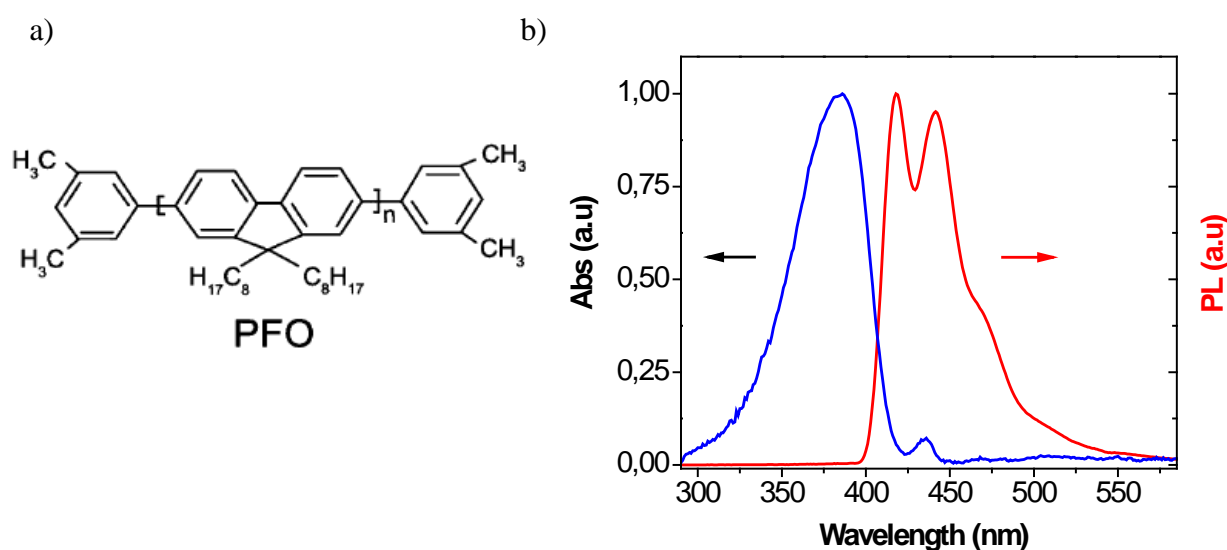


Figure.2.1 (a) The chemical structure of PFO(Ploy[9,9-dioctylfluorenyl-2,7-diyl])

(b) Absorption and Photoluminescence measurements of the PFO polymer solution

2.1.2 Commercial available SWNT solution (IsoNanotubes-S)

For device fabrication also commercial available aqueous surfactant solution which was bought from IsoNanotubes company was used. This enrichment suspension contains 95% of semiconducting species, absorption spectrum of this material is given by Fig. 2.2

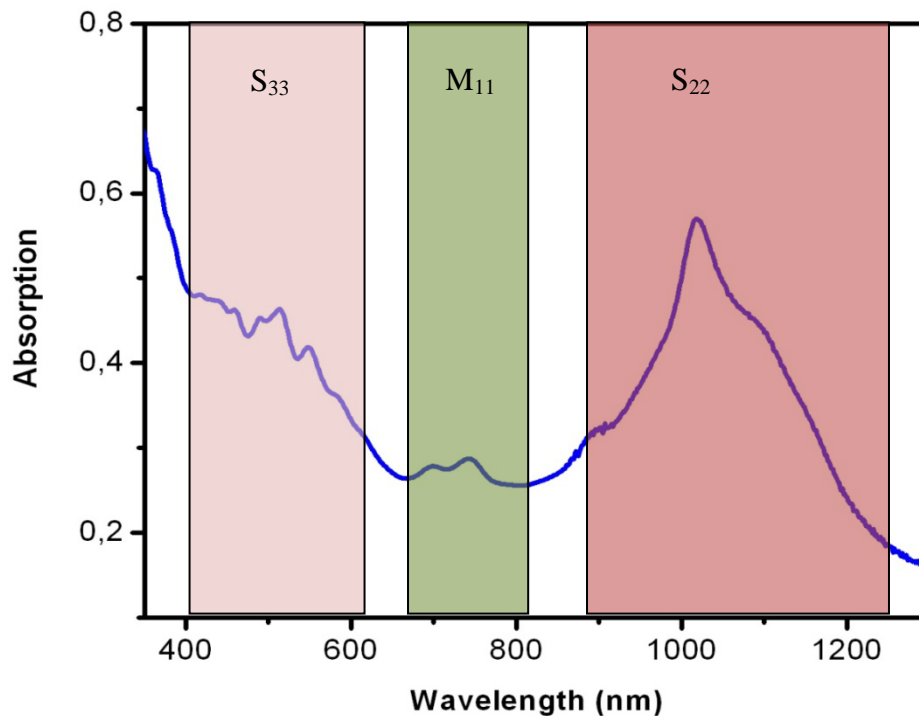


Figure. 2.2 Absorption spectra of s-SWNT solution, 95% purity of semiconducting species.

Generally it is well known that from absorption spectrum of SWNT suspension it is possible to estimate the transition energies for all nanotubes species in solution. Fig. 2.2 was taken from specifications supporting sheet from the IsoNanotubes company. Also we know from company that product product has diameter range of (1.2 - 1.7 nm).

Also from the absorption spectra at the Fig. 2.2 it is possible to distinguish metallic and semiconducting species. Several peaks from metallic and semiconducting species was shown where we would expect them: S₃₃ transitions should lie between ~450-630 nm, M₁₁ transitions between ~600-850 nm, and S₂₂ transitions between ~ 900-1,270 nm. Were peaks for metallic nanotubes are labeled as M and for semiconducting as S respectively. At the figure we can see that metallic peak are quit big comparing with semiconducting one, it proves that our product has relatively high percentage of metallic species.

2.1.3. CoMoCAT carbon nanotubes (SWeNT)

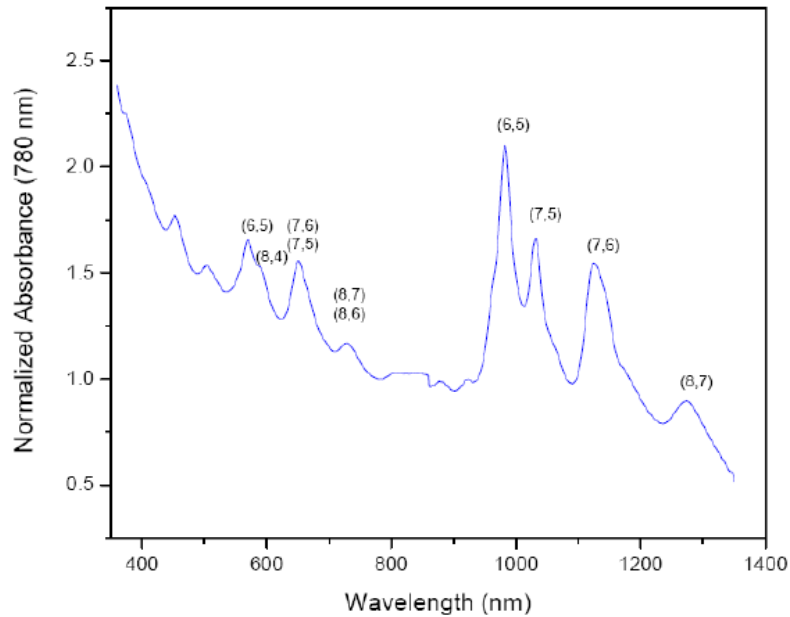


Figure. 2.3. Optical Absorption spectrum for SWeNT CG-100 product, which was used in experiment. Three dominant semiconducting species are (6,5), (7,5) and (7,6).

The SWNT product(CG-100) what was used in experiment was grown by the CoMoCAT method, made by SWeNT company. CoMoCAT method is SouthWest NanoTechnologies Inc.'s unique catalytic method that produces single-wall nanotubes of high quality at very high selectivity. In this method, SWNT are grown by using CO decomposition into C and CO₂ at 700-950°C in flow of pure CO at a total pressure that typically ranges from 1 to 10 atm. Co-Mo metals were used as a catalyst during SWCNT production by CO disproportionation. The catalyst also inhibits the sintering of Co particles. Created nanotubes have a length of several hundred nanometers and diameter in range of (0.87 ±0.3 nm). From the absorption spectrum of this material (Fig.2.3) it is possible to notice that the percentage of semiconducting species are (7,5), (7,6) and (6,5) is highest. And these species is most important for us.

2.2. Preparation of the PFO-SWNT solution

The preparation of SWNT dispersion only consists of sonication and ultracentrifuge. Before to start the preparation of PFO-SWNT solution, following materials, Poly(9,9-di-*n*-octylfluorenyl-2,7-diyl) (PFO) and CoMoCAT SWNTs powder were taken. The mixture was done with following mass ration- 1 mg of dry SWNT was added to 3 mg of PFO and 10 ml of toluene. Due to the strong Van der Waals force between nanotubes, carbon nanotubes have a strong affinity to make bundles. These bundles contain both types of nanotube, a semiconducting species and the metallic ones. For the purpose to create dispersion which contains predominantly individually dispersed nanotubes we used sonication procedure to broke the bundles, in order to improve interaction between PFO and single nanotubes but not with bundles. PFO-SWNT mixture was sonicated for 4 hours in a tabletop ultrasonic bath (VWR, The Netherlands). In terms that the system, single nanotube+PFO molecules has lower density than the system bundled nanotubes + PFO molecules, the bundled nanotubes precipitate to the bottom of the tube after centrifuge procedure, while wrapped single dispersed nanotubes are in the upper part (supernatant). After sonication, the crude dispersion was placed into the polyallomer tubes with a weight difference no greater than 1 mg and ultra-centrifuged at 45k rpm for 1 hour (Rotor: MLS-50, 217 000 g). All heavy carbon compounds and large bundles of carbon nanotubes sink to the bottom of tubes and the supernatant (50%) of dispersion was collected and transferred into new tube, then followed a second ultra-centrifuged step for 5 hours at 50k rpm (268 000 g). After the second step ultracentrifuge, the dispersed semiconducting SWNTs precipitated to the bottom of the tube, accumulating into a little but visible black 'pillet'. The 'pillet' was diluted with toluene and centrifuge procedure (1 hr, 16800 g) was repeated twice. Finally we obtained semiconductor-enriched SWNT dispersion for the device fabrication step. Fig.2.4 schematically represents all three steps of our preparation procedure of the PFO-SWNT solution.

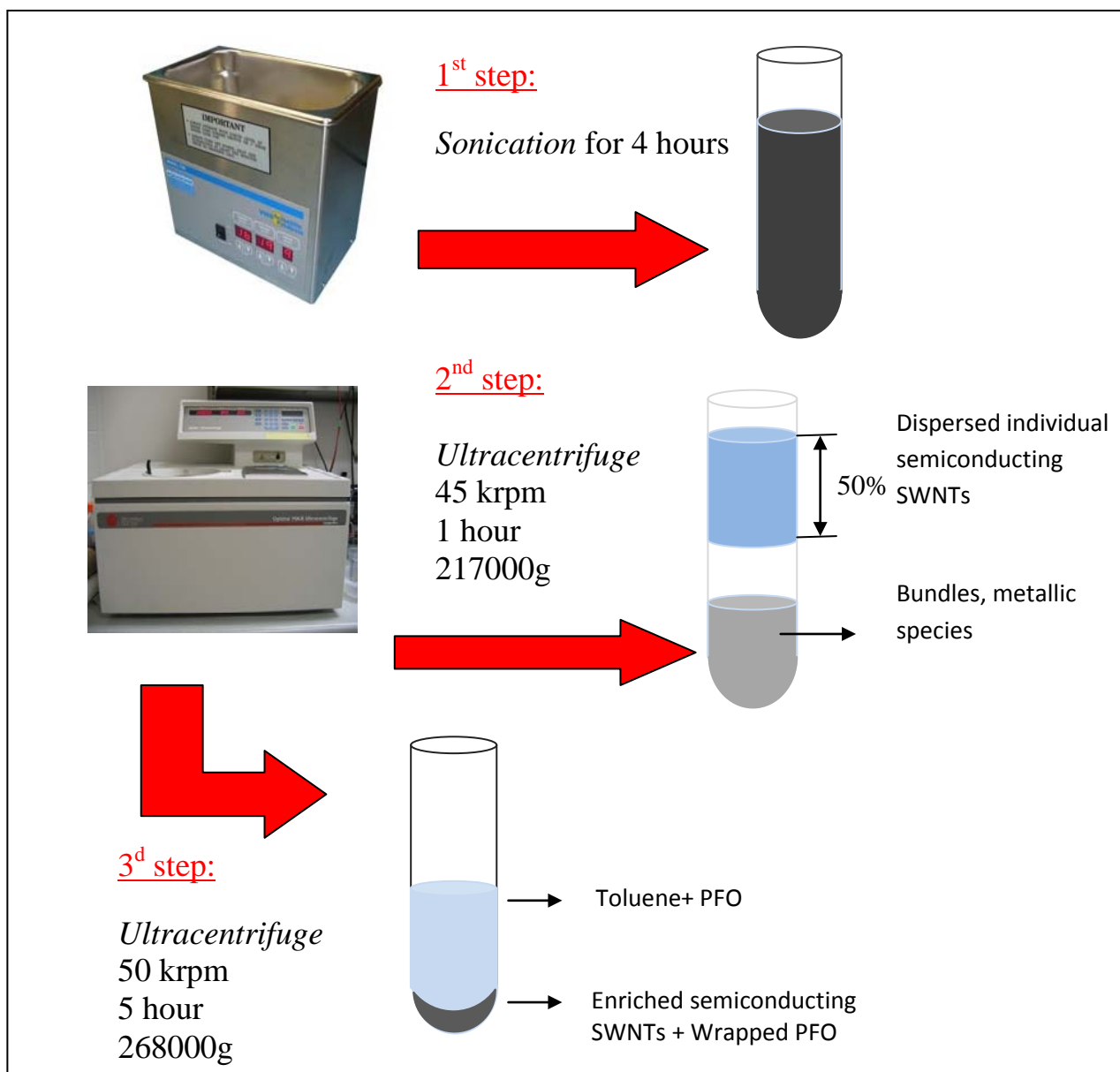


Figure 2.4. Schematic representation of preparation procedure of the PFO-SWNT solution.

2.3. Optical Characterization

Absorption spectra of the prepared SWNT suspension was measured by using a Perking-Elmer UV – vis-near-infrared spectrophotometer (Lambda 900). For the PL measurements, the SWNT dispersion was excited at 760 nm by a 150 fs pulsed Kerr mode locked Ti-sapphire laser and measured with InGaAs detectors. The spectra was calibrated for the instrumental response.

2.4. The substrate



Figure.2.5. Schematic device structure with bottom-contact geometry

SWNT FETs were fabricated by using drop-cast method. The SWNT solution was coated on bottom-gate/bottom-contact substrates (Fig.2.5) A heavily doped Si substrate served as the gate electrode and thermally grown SiO₂ was used as the dielectric layer (230 nm thickness). The source and drain electrodes consisted of 10 nm of Ti and 30 nm Au.

2.5. Device Fabrication

During device fabrication step two types of devices were done. Firstly transistors based on commercial available (IsoNanotubes) aqueous SWNT suspension were made. The second set of devices was made using our “home made” suspension. The difference in preparation between these two sets of devices is only in difference of coating method of the SWNT solution on the device surface. For commercial available solution spin-coating procedure was used while for our “home made” suspension we used drop cast method. All the substrates were first cleaned in an ultrasonic bath using acetone and isopropanol for 10 min each, and then rinsed with deionized water. Next, the substrates were put in an oven at 140⁰ C for 10 minutes and cleaned with a UV–ozone treatment for 20 minutes to remove organic contaminants from the surface. Prior to coating of SWNT dispersion, substrate-surface was modified with 3-aminopropyltriethoxysilane (APTES: Sigma-Adrich) in order to increase the adhesion of SWNTs , the APTES-assisted deposition is shown in Fig. 2.6.

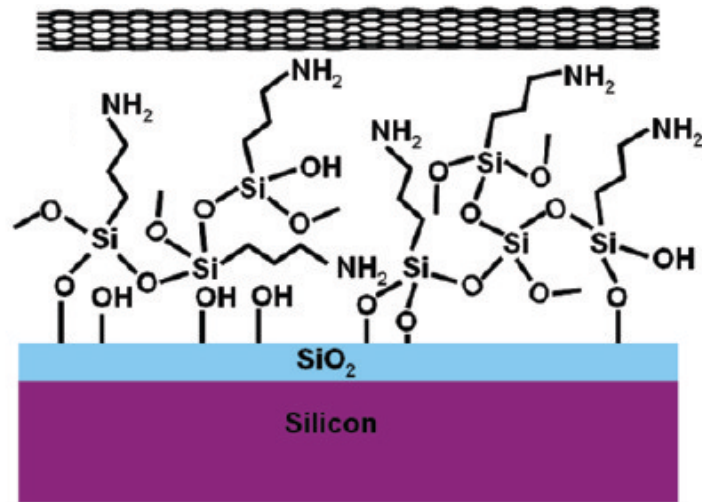


Figure 2.6. Schematic diagram of APTES assisted nanotube deposition on Si/SiO₂ substrate.

The modification procedure with APTES treatment follows as: the cleaned wafer is immersed into diluted APTES solution (3 drops of APTES in 20 mL of Toluene for 8 hours, then rinsed with Toluene, Acetone and Propanol and finally blown dry thoroughly. The substrate then was put on a hotplate at 60⁰, the concentrated SWNT-semiconducting solution was drop casted on the substrate. After the deposition, the substrates were annealed in a vacuum oven at 150⁰ C for eight hours. The annealing process needed to improve the connection between the contacts on substrate and carbon nanotube network.

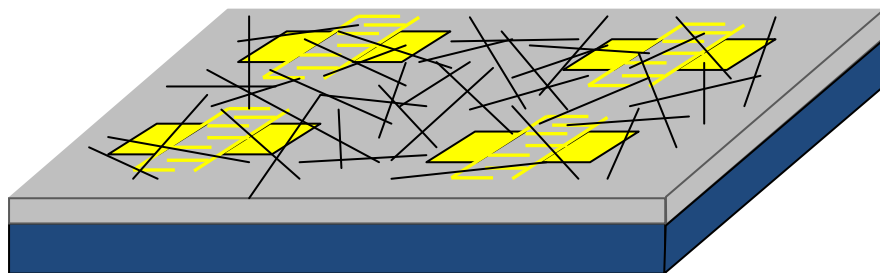


Figure.2.7. Schematic illustration of the device fabrication. Enriched SWNT solution drop-casted on the substrate surface.

The performance of the carbon nanotube network transistor will be described in the next chapter.

2.6. I-V characteristics measurements

Electrical characterization of transistors based on commercial available solution (IsoNanotubes-S) and PFO - SWNT dispersion was measured in a home-built probe station under high vacuum pressure (10^{-6} mbar) and also in air atmosphere with a Keithley 4200 semiconductor analyzer at room temperature. Mica sheet was put in between of the holder and silicon substrate to isolate the device and to prevent parasitic currents. The applied drain-source and gate bias was scanned in a range from -50 to 50 V. The device mobility was calculated from the drain-source current (I_D) versus the gate voltage (V_G) using standard formulas:

$$\mu = \frac{2L}{WC_i} \left(\frac{\partial \sqrt{I_D}}{\partial V_G} \right)^2 \quad (1.1)$$

and

$$\mu = \frac{L}{WC_i V_D} \left[\frac{\partial I_D}{\partial V_G} \right] \quad (1.2)$$

for saturation and linear regime respectively, where L and W are the channel length and width defined by the patterns of electrodes C_i is the capacitance per unit defined by the thickness of the SiO_2 .

2.7. Microscopy

Atomic force microscopy was used to characterize of the SWNT coverage of the device channel and was performed using Digital Instruments – Veeco Nanoscope IV Multimode AFM setup. The images were acquired in the tapping mode. Ultra sharp (Veeco Model SNL-10) tips with diameter in a range from 10 to 2 nm and the resonance frequency 75 kHz and force constant of 0,58 N/m were used. Scanning electron microscopy (JEOL) was used to image the device channel at accelerating voltage of 10 kV.

Chapter 3

Results and Discussion

In this chapter, the results of the PFO-SWNT suspension preparation and field effect transistors fabrication will be given and discussed. Firstly, we will discuss the device that was fabricated using commercial available aqueous suspension (95 % Nanointegris product). Secondly we will discuss our procedure of preparation of enriched SWNT dispersion by semiconducting species, particularly the CoMoCAT SWNTs suspension sorted by PFO wrapping to purify the semiconducting sample will be discussed. The last section of the chapter will deal with the device fabrication of the SWNT network transistor and particularly with the performance of the device itself. Parameters of transistor such as mobility, on/off ratio will be calculated. According to the SEM image of the channel of the device, will be estimated the coverage of the nanotube networks and effective mobility will be calculated. Also mobility and on/off ratio will be compared for different ambient regimes. At the end ambient effect will be discussed in detail.

3.1 SWNT suspension

3.1.1 Commercial available SWNT suspension

As was mentioned early in device fabrication two types of SWNT suspension were used. Firstly commercial available aqueous surfactant suspension was used in experiment. Absorption spectrum which represent electrical properties of this material was shown in Chapter 2 (see Fig. 2.2)

3.1.2 PFO and CoMoCAT mixture

Firstly, we did absorption measurements to estimate purity of our “home made ” suspension. Figure 3.1 shows the measured absorption spectrum of the wrapped carbon nanotubes. Blue line defines as-dispersed SWNTs and red line corresponds to the enriched semiconducting SWNTs.

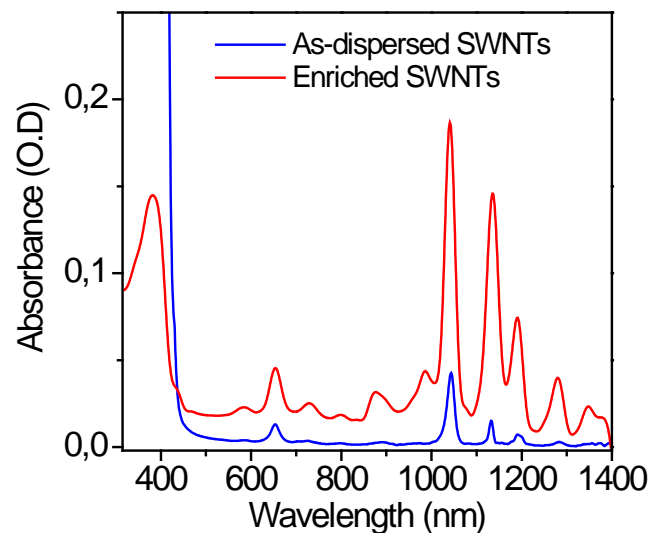


Fig. 3.1 Optical absorption spectra of the as-dispersed SWNTs (blue curve) and the enriched SWNTs (red curve) in toluene solution.

PFO in toluene solution has proven to be one important candidate for sorting semiconducting SWNTs due to the unique interaction between polymers and carbon nanotubes [16,17,18]. The absorption spectrum of the as-dispersed SWNTs (blue) shows almost no background intensity. The peaks at wavelength higher than 900 nm are the E_{11} transition of 4 semiconducting SWNT species corresponding to (7,5), (7,6), (8,6) (8,7). The absorbance below 400 nm is from the polymer (PFO) in the solution with concentration close to that of the pristine solution (~0.3 mg/ml). The absorption spectrum of the SWNTs after enrichment (red) shows much higher absorbance intensity (O.D. ~ 0.2) than that of the as-dispersed one (O.D. ~ 0.05). By taking into account the absorption cross section $\alpha(E_{11}^S) \approx 1 \times 10^{-18} \text{ cm}^2 / \text{atom}$ for dispersed carbon nanotubes [36], we estimated their concentration to be about 0.4 $\mu\text{g/ml}$ for the as-dispersed SWNTs and 6 $\mu\text{g/ml}$ for the one after

enrichment. No optical transitions from metallic species in the spectral range of 500-600 nm were observed. The reduction of absorption intensity at 380 nm is as much remarkable, which indicates a high efficiency of this method for the removal of excess polymer from the dispersion. There have been several reports on the preparation of semiconducting SWNT dispersion by using conjugated polymers so far. Izard et al. reported the separation of dispersed SWNTs with excess PFO by extensive washing [37]. However, the efficiency of the separation and the yield of the procedure for SWNT enrichment were not mentioned in details. Krupke et al. reported the realization of carbon nanotube device array by using PFO/toluene dispersed SWNTs but no efficient method for the removal of wrapped polymers was presented [38]. Chan-Park et al. demonstrated a degradable conjugated polymer for the enrichment of semiconducting SWNTs but the selectivity is not as good as that of PFO [39]. Arnold et al. presented the method for the preparation of semiconducting SWNTs analogues to what we used in this study [40]. However, our procedure is much less time-consuming with the aid of ultracentrifugation. Also to prove that our suspension has a high purity of semiconducting species, measurements of the finite frequency (GHz) electrical conductivity of our suspension was done. This measurements showed that our suspension has a purity 98%-99% of semiconducting species.

3.2 Device Performance

As was discussed above in current work two types of field effect transistors was produced using solution processed individual carbon nanotubes. Firstly we used commercial available aqueous surfactant suspension. Secondly our “home made” enriched semiconducting SWNT suspension was used. Concerning fact that concentration of nanotubes in commercial available suspension was higher than in “home made” one we used two different method of fabrication. In case of commercial available suspension we used spin-coating technique and during experiment with commercial available suspension we used several spin-coating programs with different speed and tried to find the optimal one to achieve the best transistor performance. In total near 300 devices were made with 5 different spin-coating programs. All devices was measured in vacuum atmosphere. In second part of the project devices based on “home made ” suspension were fabricated. During fabrication procedure drop cast method was used and near 50 devices were produced. It is necessary to say that drop casting method was successfully used to distribute the carbon nanotubes on the substrate. The annealing process is necessary to make the device work. The device mentioned above was also measured when the substrate had not been annealed. Only short circuits and no connections were found along with small traces of metal behavior. The influence of the annealing process was investigated and effects of recovering annealing after expositions devices in the air atmosphere were investigated. AFM and SEM microscopy was used to investigate magnitude of coverage of the channel of transistor and estimate magnitude of the effective mobility of charge carriers.

3.2.1 Device based on commercial available solution

Before the fabrication SWNTs based on our “home made” suspension was made, we firstly fabricated set of devices based on commercial available suspension. Concerning the fact that the purity of commercial available suspension is near 95% of semi-conducting species and that the concentration of nanotubes in suspension is high it is obvious that for fabrication procedure it is necessary to use spin-coating technique. In experiment we tried to find optimal speed to get the best device performance. At the schematic drawing (Fig 3.2) it is clear to see that for low spin speed of the substrate we will have relatively high coverage on nanotubes in the channel and concerning the fact that we have a big percentage of metallic SWNT. As a consequence the probability to have metallic species in percolation channel is so huge, it means that the probability to have short circuit device is also high. In other words the chance to create a semiconducting connection between the source and drain without also creating a metallic connection is very small. For high rotation spin speed we will have opposite situation, the SWNT coverage of the channel will be so small and as consequence the probability to have semiconducting percolation channel also will be small and in this case we will have so small source drain current. This fact leads that the chance to create a semiconducting connection between the source and drain is small.

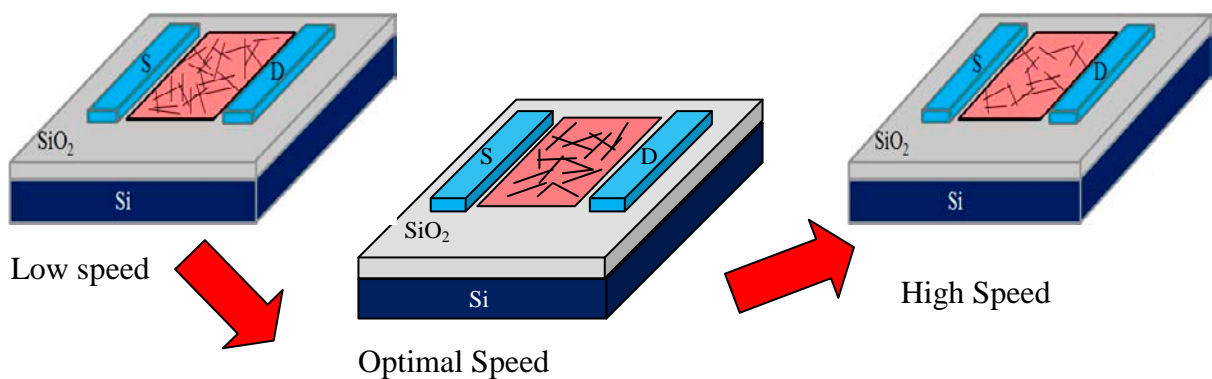
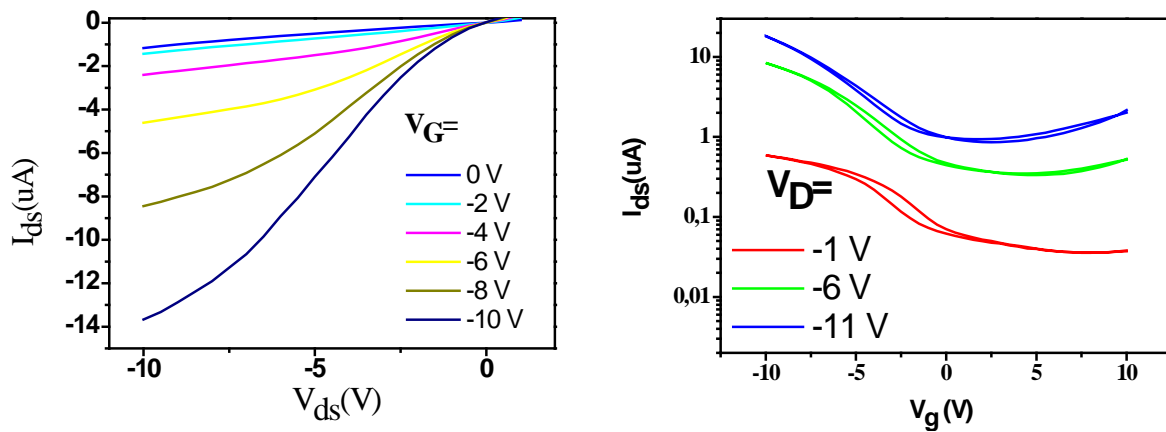


Fig 3.2. Schematic drawing of experiment. Dependence of SWNT coverage versus rotational speed is depicted.

Generally speaking, as commercial available suspension is aqueous surfactant suspension, devices fabricated from this product are unipolar transistors only with p-type behavior. However, the transport of electrons in other words n-type character is strongly suppressed and in our case it is possible to say that it is completely absent. The origin of the absence of electron transport as was mentioned in the introduction part is still unclear. One of the possible explanations could be that electron injection is prevented due to Schottky barriers at the metal/SWNT interface [41]. But the best explanation of this issue could be that was given by Martel [42]. It was demonstrated that oxygen and water as a couple could suppress electron conduction in SWNTs dramatically like in the case of organic semiconductors.

The performance for a device with a channel length of 20 μm is shown in Fig 3.3. Obviously, this device is unipolar with p-type character of the charge carriers. The apparent mobility is near

$10^{-2} \text{ cm}^2 \text{ V}^{-1} \text{ s}^{-1}$. The mobility was calculated using equation (1.1) and (1.2). Also as can be seen from the transfer characteristic that On/Off ratio only is near the 10.



Channel Length	On/Off ratio	μ ($\text{cm}^2/\text{V}^{-1} \text{ s}^{-1}$)	V th
20 μm	10	$17 \cdot 10^{-3}$	- 4 V

Fig 3.3. The output and transfer characteristics of the of SWNT transistors based on commercial available solution when spin-coating speed equals to 700 rpm. The channel length of the device is 20 μm . Magnitude of the hole mobility and average on/off ratio one are listed in the table the figure.

In generally, low on/off ratio could be explained by relatively high probability of percolative transport through metallic nanotube networks due to the high percentage of metallic nanotubes. However, on/off ratio of device with small channel length will be so small because commercial available suspension contains a big amount of metallic species and on/off ratio parameter also suffers from this. These suspension is not applicable for short-channel SWNT FETs. In the same way it is possible to explain relatively high mobility of holes. Because SWNT FETs strongly depends on the presence of metallic tubes in the percolation path. For example if we have two SWNT suspension with different percentage of semiconducting content, it is obvious that the device which was fabricated with higher purity semiconducting SWNTs suspension will have lower mobility that the device that was fabricated using suspension where percentage of semiconducting content is lower. However, the nanotube coverage is proportional to the number of percolation path in FETs and determines device characteristics, so we will estimate the coverage of SWNTs in the channel region. As easily to understand that in our case coverage of SWNTs network in the channel proportional to the spin speed magnitude during spin-coating procedure, we found the optimal coverage of the SWNTs network changing spin speed. Statistical study of the finding

procedure of the optimal spin-coating speed can be seen in the Fig 3.3. One can say that the optimal magnitude of the speed is near 700 rpm. For all devices with different channel length (20 μm , 10 μm , 5 μm) general trend was the same, when the speed was near 700 rpm, devices with different length had maximal magnitude of the mobility (Also see Appendix A).

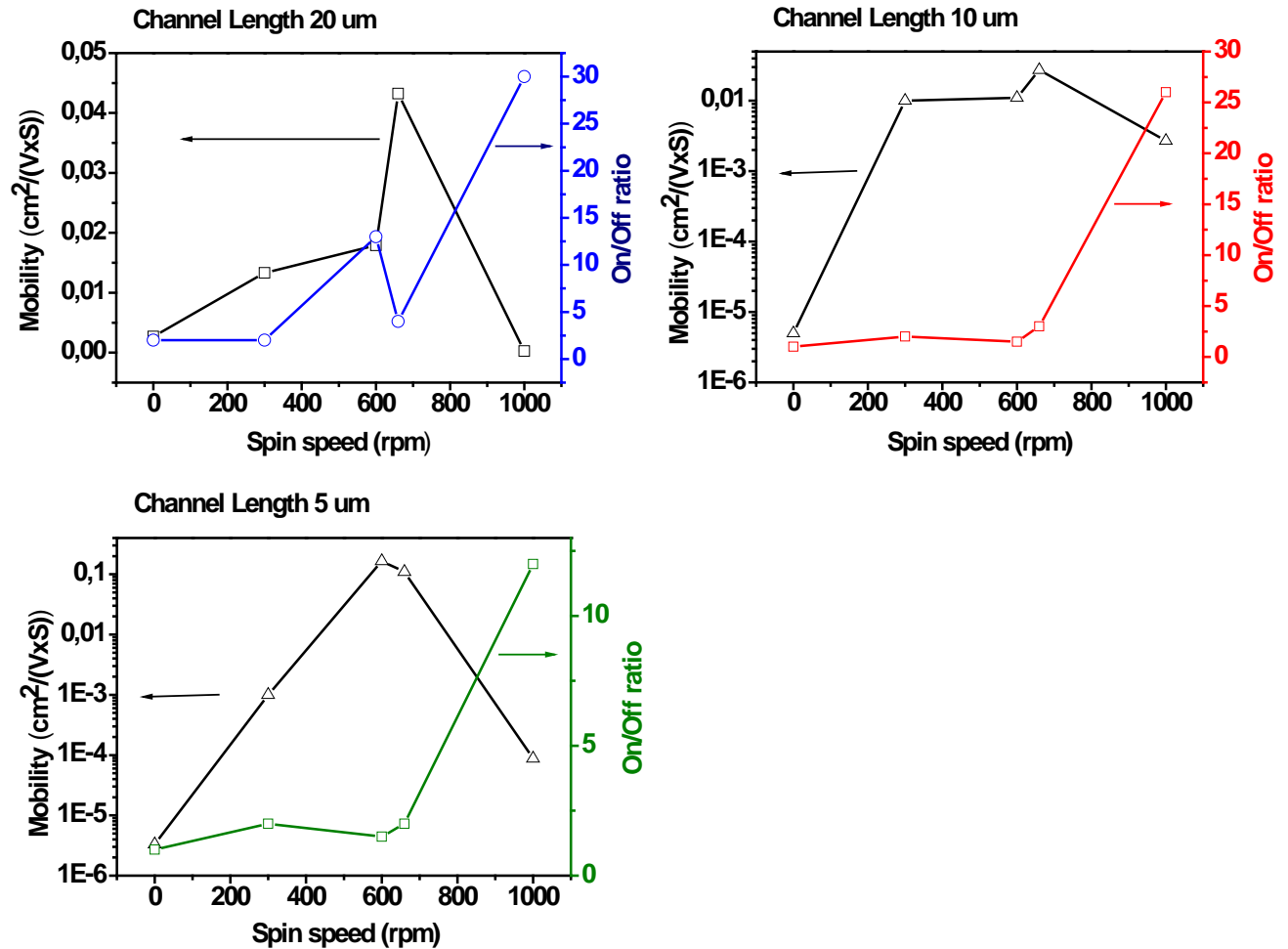


Fig 3.4. Statistical study of the electrical characteristics of SWNT transistors based on commercial available solution . Plots of hole mobility and average on/off ratio versus device channel length.

General trend explains: when we have low spin speed our SWNT coverage is huge and as consequence we have a lot metallic tubes in SWNT networks and we short circuit device. When we have to high speed, the probability to have percolate channel is small and probability to have situation when we have no semiconducting connection between source and drain is high and as a result we have no transistor at all. But in case when we have a high spin speed it is clear to see that on/off ration increasing and mobility is smaller than for middle “optimal” speed. It means that in percolation channel we have small amount of metallic tubes. But it is necessary to say that for word “optimal speed” it means that for speed 700 rpm most of fabricated devices are working and have decent performance. One can mention that when 1000 rpm fabricated transistor gas better on/of ratio value, but main drawback is that when the spin speed is so high, probability to have working device is small. So for this experiment with commercial available solution we proved statement that SWNT

FETs strongly influenced by the presence of metallic tubes in the percolation path and secondly the coverage of SWNTs in the channel region is also important.

3.2.2 Device based on “home made” solution.

In this paragraph the results of the devices based on “home made” suspension will be discussed. One can say that using higher purity semiconductive enriched nanotubes suspension, on the one hand it can help to achieve sufficient on/off ratio with smaller channel length, thus smaller device area; on the other hand, since higher purity requires more ultracentrifugation and sonication procedure time, which will give rise to shorter nanotube length, it can cause more nanotube percolation and hurt the mobility of the devices. It is obvious that for different channel lengths device will show different performances. For channel length 20 and 10 μm we should have better performance than in range 5 and 2.5 μm , because for small channel length the probability to have short circuit due to the presence metallic species is much higher. As was mentioned above near 50 devices was made using drop cast method. One should note that for instance comparing with devices which were made based on commercial available we used dropcast because in case of “home made” suspension concentration of nanotubes in solution was less than in commercial one, so in terms to increase total nanotube coverage of the effective channel of the device we used dropcast technique instead of spin-coating. Firstly all created devices was measured in vacuum and it is obvious that the rising curve in the transfer curve is used to calculation mobility, since this curve represents the intrinsic mobility of the device the most accurate. In order to improve the density and uniformity of the solution-based nanotube assembly, aminosilane is introduced due to its well-known affinity to the carbon nanotubes. In this work, aminopropyltriethoxy silane (APTES) is used to functionalize the Si/SiO₂ surface to form amine-terminated monolayer and the schematic of the APTES-assisted deposition is shown

Because that the coverage is proportional to the number of percolation path in FETs and determines device characteristics such as mobility so we will look more detail for this issue below.

3.2.3 Vacuum measurements.

The typical performances of the carbon nanotube transistors with channel length 20 μm and 10 μm can be seen in Figure 3.3 and Figure 3.4 respectively, it is obvious that devices shows ambipolar behavior.

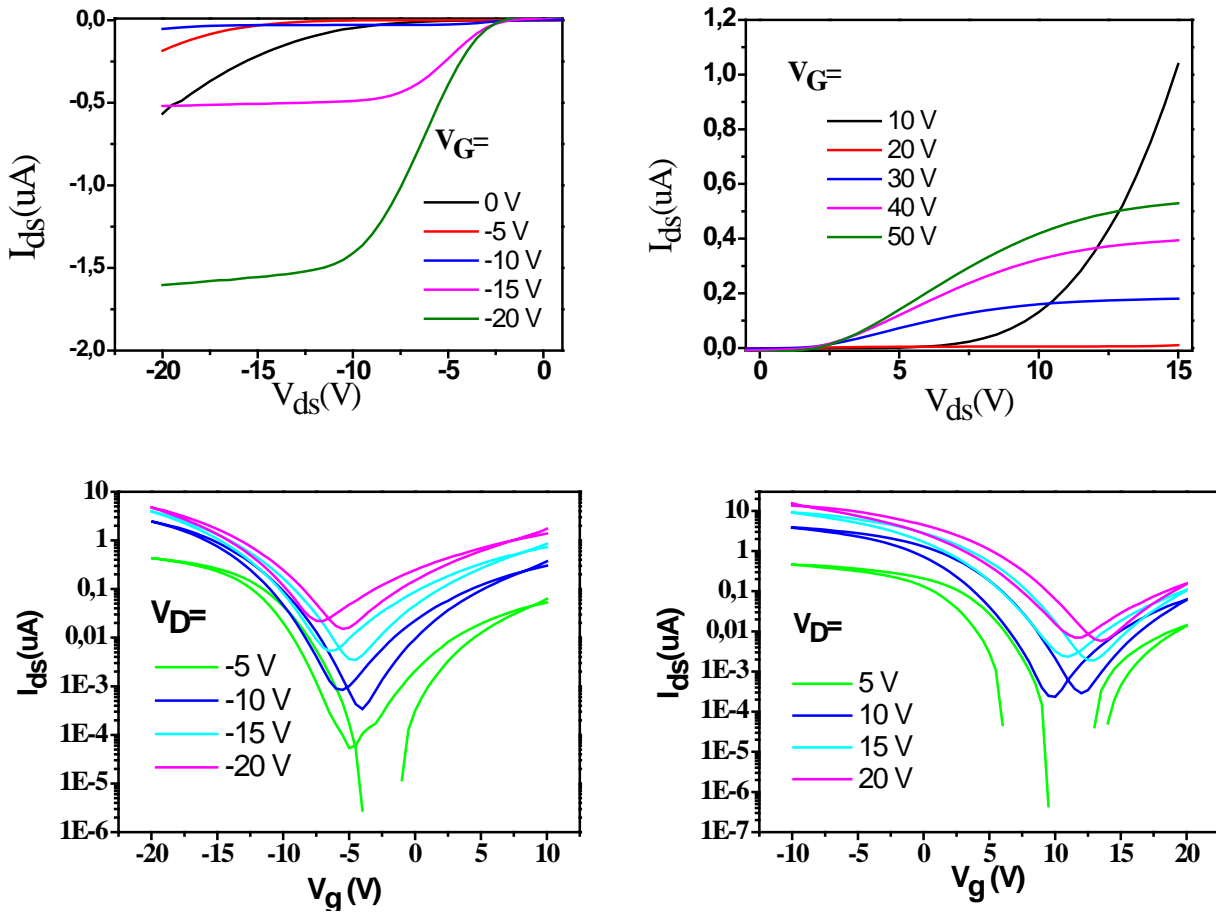


Fig. 3.3 The output and transfer curves of a typical ambipolar field effect transistor based on the semiconducting enriched carbon nanotube suspension. The channel length of the device is 20 μm , the width 1 cm .

As clearly can be seen that the magnitude of on/off ratio for p channel is in range of 10^4 and for n-type channel near 10^3 . One should note that on/off ratio of all devices is comparable to the prepared with 99% semiconducting SWNT solution [43].

It is necessary to mentioned that for device with channel length 10 μm , on/off ratio decreased and mobility increased which is agree with explanation that was mentioned previously.

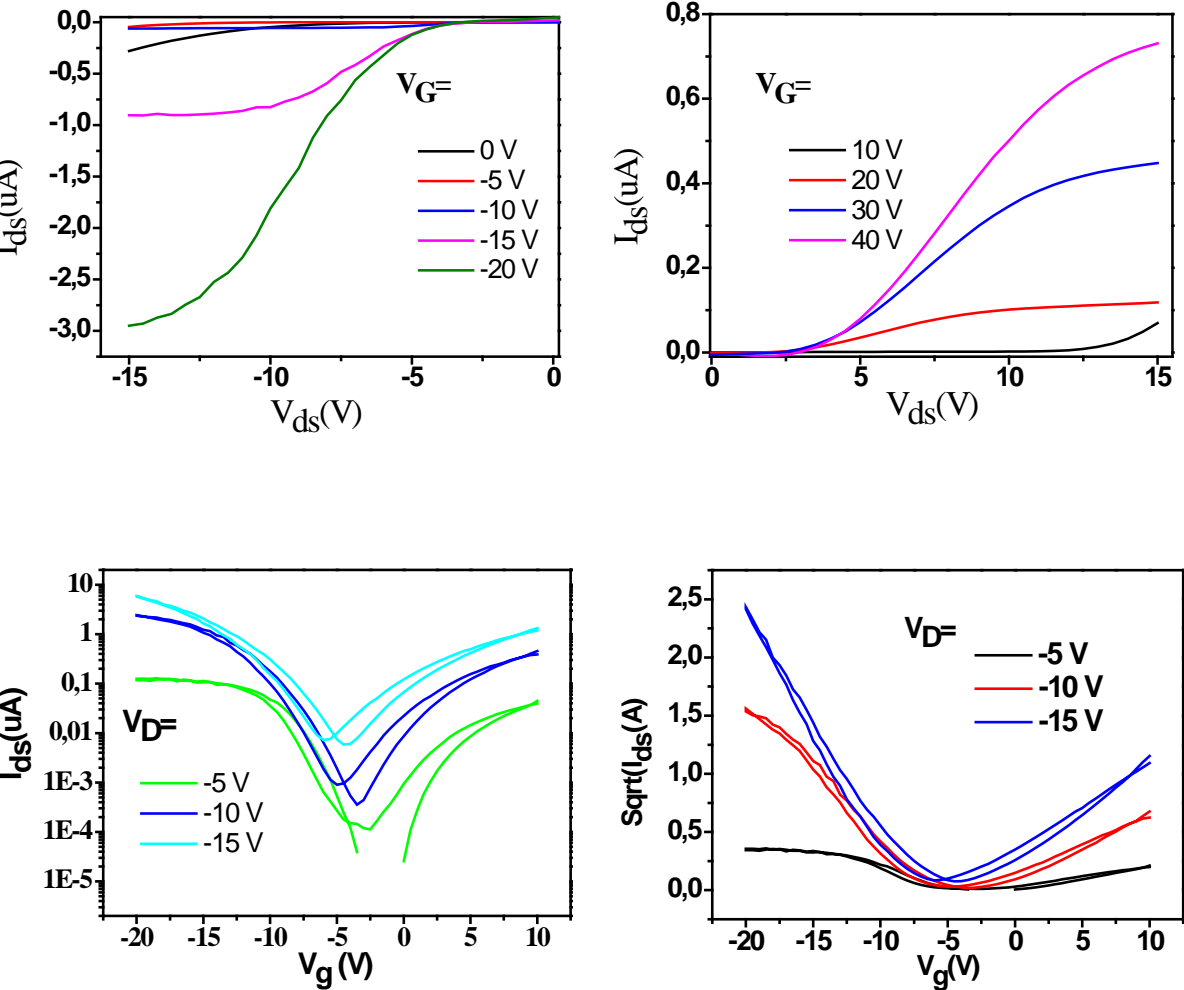


Fig. 3.4. The output and transfer curves of a typical ambipolar field effect transistor based on the semiconducting enriched carbon nanotube suspension. The channel length of the device is 10 μm , the width 1 cm.

In total than 10 devices were measured at each channel length. The device mobility is calculated by using the standard formula for saturation and linear regime (1.1) and (1.2) respectively for field-effect transistors and the value for channel width (W) and length (L) is from the pattern of the electrodes.

3.2.4 Mobility and on/off ratio calculation.

Typical I-V curves of ambipolar transistor was shown in previous section (Fig. 3.3 and Fig. 3.4). Using transfer characteristics we will calculate mobility of charge carriers for both p and n channel. For example we will show two examples of calculation hole mobility in case of linear and saturation regimes.

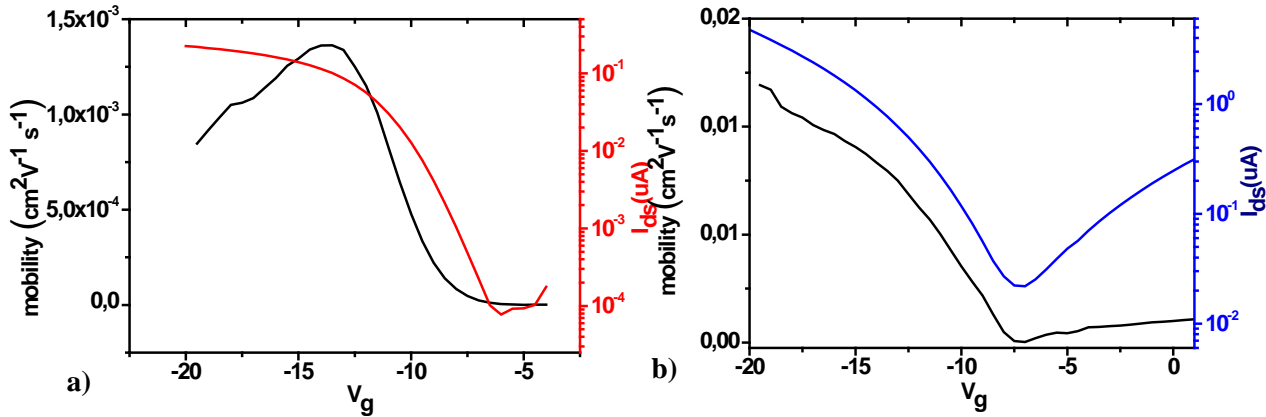


Figure 3.5 a) Transfer characteristics of device with channel length 20 μm showing dependences of I_{SD} and the mobility on the linear regime $V_{\text{d}} = -5$ V. b) Same trend but in case on the saturation regime $V_{\text{d}} = -20$ V.

The transfer characteristic for p-type channel on the linear regime of the device with channel length 20 μm are illustrated in Fig 3.5.a (black line). The mobility in linear regime shown in Fig 3.5a (red line) and it is determined using the equation (1.1) as can be seen from the plot the peak mobility of the device is $1,4 \times 10^{-3} \text{ cm}^2 \text{ V}^{-1} \text{ s}^{-1}$. Similar plotting and calculation we did with saturation regime but for calculation of the mobility magnitude we used equation (1.2) and as one can see from the Fig.3.5b the maximal value of the mobility in saturation regime is near $10^{-2} \text{ V}^{-1} \text{ s}^{-1}$. The same procedure was done with device which has channel length 10 μm . We did mobility calculation for linear and saturation mobility. We could see from Fig 3.5, mobility dependences versus gate voltage show similar trend as was in case of channel length 20 μm . The peak of the linear mobility is $7 \times 10^{-4} \text{ cm}^2 \text{ V}^{-1} \text{ s}^{-1}$ and saturation mobility is $8 \times 10^{-3} \text{ cm}^2 \text{ V}^{-1} \text{ s}^{-1}$. Of course it is difficult to understand general trend of dependence mobility versus channel length comparing only these two devices. Because it is possible to say that our method of fabrication of FETs in some sense is probabilistic, we cannot control the coverage of active channel of the transistor by SWNT network using drop cast method. So in respect that two same devices can have different SWNT coverage and concentration of the metallic tubes it is very necessary to do statistical study of SWNT FET performances and below we will do that.

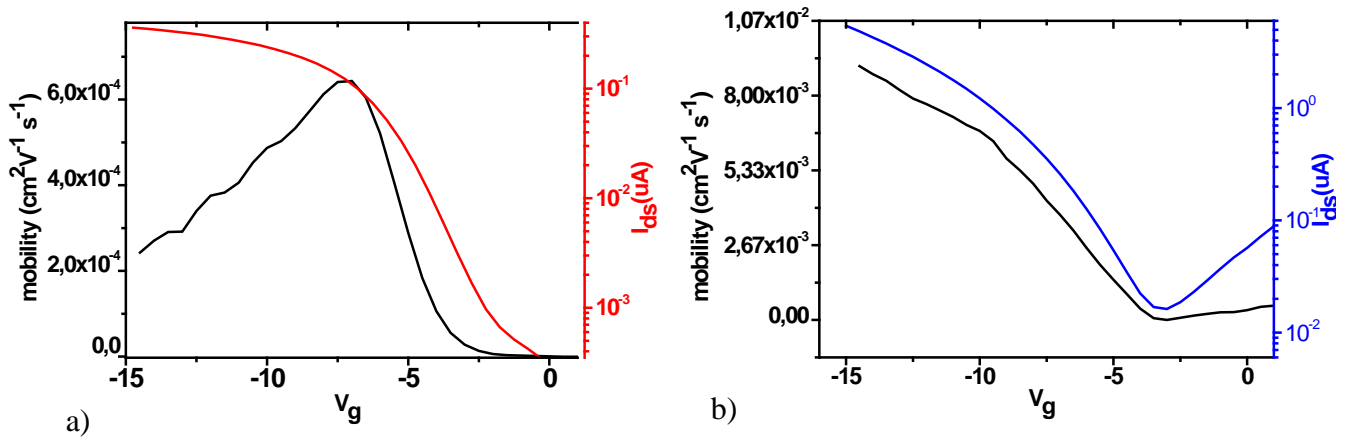


Figure 3.6. a) Transfer characteristics of device with channel length 10 μm showing dependences of I_{SD} and the mobility on the linear regime $V_d = -5$ V b) Same trend but in case on the saturation regime $V_d = -15$ V.

Figure 3.7 shows the statistical study of the electrical characteristics of bottom-contact FETs with randomly distributed SWNT network as channel.

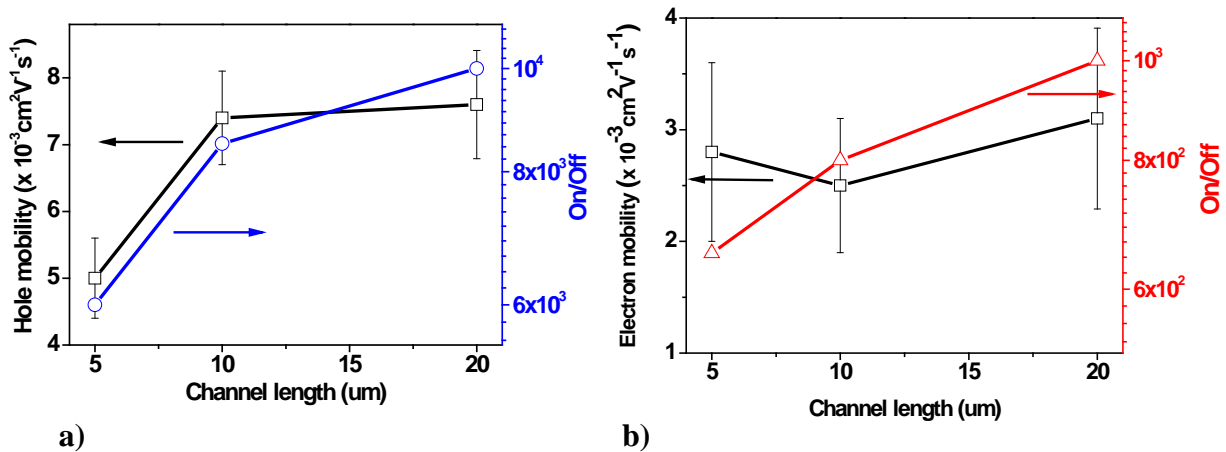


Figure 3.7. Statistical study of the electrical characteristics of SWNT transistors: a) Plot of hole mobility and average on/off ratio versus device channel length; b) Plot of electron mobility and average on/off ratio versus device channel length.

The values for channel width (W : 1 μm) and length (L : 5, 10, 20 μm) are defined by the pattern of the electrodes. Hole mobility (μ_h) is in the range of $5-8.5 \times 10^{-3} \text{cm}^2 \text{V}^{-1} \text{s}^{-1}$ and electron mobility is $2-4 \times 10^{-3} \text{cm}^2 \text{V}^{-1} \text{s}^{-1}$, respectively. Device mobility remains almost constant and on/off ratio increases with the increase of the channel length. Such channel-length dependent characteristics was reported in previous reports and has been explained as the result of metallic tube residual or tube-tube junction. In order to that our suspension has higher semiconducting purity we could neglect in this study contribution from metallic tubes. It is possible to say that we have channel-length dependent device performance mainly due to the intertube coupling resistance and this resistance is much higher than in case of single nanotube. The device mobility is limited by the percolative transport through nanotube

network. As the device channel length increases from a value comparable to the nanotube length to a much larger value, there are significantly more tube to-tube junctions introduced into the conduction path, causing the device mobility to decrease. But in case of other devices, device mobility is likely to be limited by the metal/nanotube contacts. As the channel length increases, the effect of metal/nanotube contacts become less significant and the mobility increases. For transistors of small channel length, would lead to less nanotube-nanotube junctions and consequently higher mobility. But in our experiment we have not so big variation of channel length that's why it is difficult to explain in good way in experiment mobility for holes and electrons shows almost constant behavior. The off current is in the order of 10^{-10} Ampere at source drain bias ($V_d = -5$ V) and on/off ratio of all the devices is in the range of 10^3 - 10^4 for p channel and 6×10^2 - 10^3 for n channel, which is comparable to that prepared with 99% semiconducting SWNT solution [43]. It indicates the high purity of the semiconducting SWNT dispersion and is also in good agreement with that estimated from optical measurements. However, two points have to be stressed here for the evaluation of SWNT FETs: the coverage of SWNTs in the channel region and the concentration of metallic tubes in SWNT network. The nanotube coverage is proportional to the number of percolation path in FETs and determines device characteristics. On the other side, conduction in SWNT network is strongly influenced by the presence of metallic tubes in the percolation path. For example, if we compare current experiment with previous one we will see that FETs prepared with 95% semiconducting SWNTs show even higher device mobility than that prepared with higher purity semiconducting SWNTs (99%) by taking advantage of a certain amount of metallic species in channel [44]. However, on/off ratio of device is sacrificed and is not applicable for short-channel SWNT FETs.

As we already mentioned before nanotube coverage is proportional to the number of percolation path in FETs and determines device characteristics. Further we did SEM and AFM measurement to estimate coverage of our active channel.

3.2.5 AFM and SEM Measurements

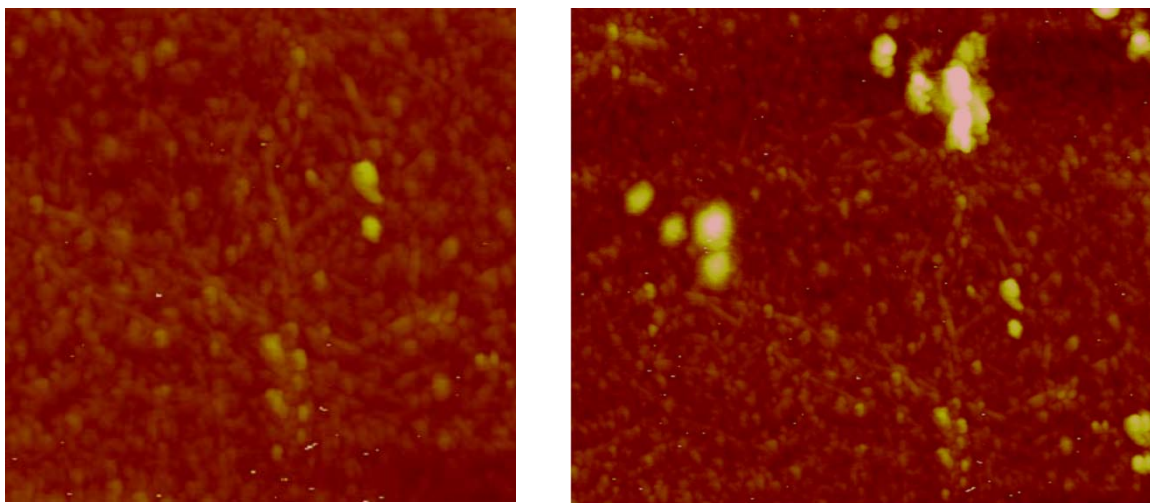


Figure 3.8. AFM measurements demonstrate of the device channel region

The channel region was investigated under AFM microscope. The topographic picture of it is shown in Fig.3.8. Unfortunately, the quality of picture is not so great, but several structures like lines-line structures are visible as well which might correspond to carbon nanotubes. However of course from this picture it is possible to see SWNT network but to make estimation about coverage of the channel it is extremely difficult task because from these pictures we could obtain only limited information. So we decided to do another experiment and to use SEM microscopy. Fig. 3.9 shows SEM images of the device channel region and it shows visible nanotube network in the device channel.

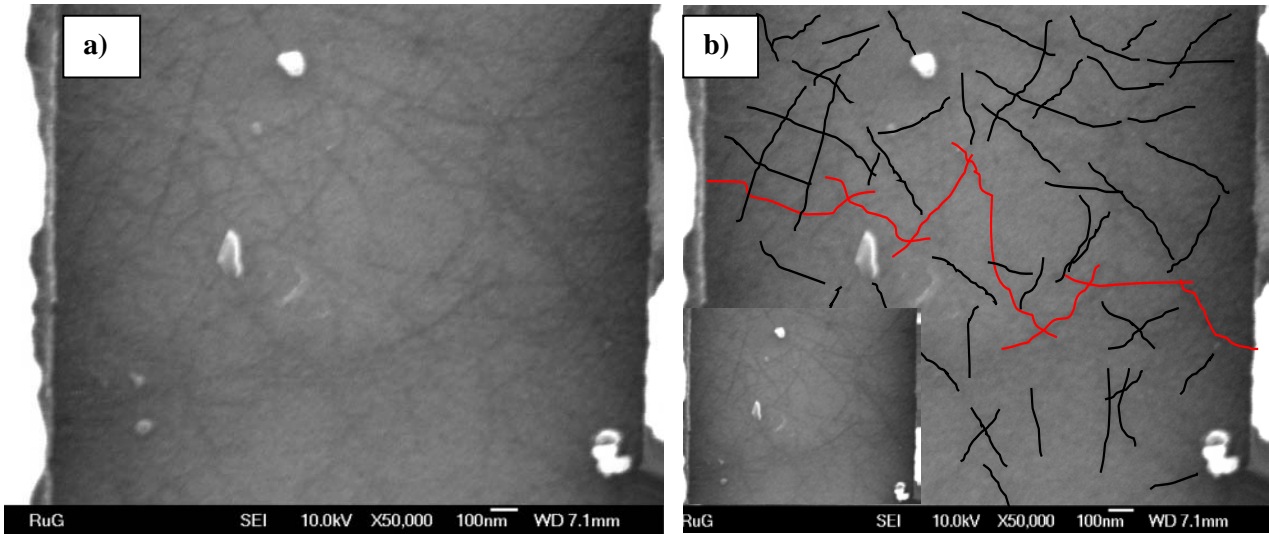


Figure. 3.9 a) Original SEM images of the device channel region b) Same image but SWNT network was emphasized for convenience.

3.2.6. Effective mobility calculation

In this study the coverage of SWNTs ($< 1\%$) is much lower than those in other reports [45] and its influence on the extraction of effective mobility will be discussed below. The coverage of the SWNTs was estimated using Figure 3.9. It equals in the range of 0.5-1% and is indicating a much higher effective mobility μ_{eff} compared to the device mobility demonstrated above. μ_{eff} can be extracted by taking into account of the coverage of SWNTs in the channel region and the effective gate capacitance C_{eff} that differs from the sheet capacitance of the dielectric layer [46]. We estimated the effective channel width to be around 1% of the channel width based on the coverage of SWNTs. By taking into account the realistic electrostatic coupling between nanotubes and gate electrode, we recalculated C_{eff} using the following equation [47,48]

$$C_{eff} = \left\{ C_Q^{-1} + \frac{1}{2\pi\epsilon_0\epsilon_{ox}} \ln \left[\frac{\Lambda_0}{R} \frac{\sinh(2\pi t_{ox} / \Lambda_0)}{\pi} \right] \right\}^{-1} \Lambda_0^{-1} \quad (1.3)$$

Where Λ_0^{-1} stands for the density of SWNTs (3-4 tubes/ μm), C_Q is the quantum capacitance of nanotube, ϵ_{ox} is the dielectric constant of SiO_2 , t_{ox} is the oxide thickness (230 nm) and R is the diameter of the nanotube (in average 0.9 nm). The effective capacitance was calculated to be 2.1 nF/cm^2 . We could therefore extract the effective mobility (μ_{eff}) around $6 \text{ cm}^2/\text{V s}$, almost three orders of magnitude higher than the device mobility shown above. Very recently, Okimoto et al., reported the relationship between device performance and the coverage of SWNTs in channel region [49], which is analogous to the thickness dependence of device performance in organic transistors [50,51]. It is reasonable to expect further improvement of device performance by increasing SWNT coverage and the efforts are currently underway.

3.2.7. Ambient effect

One of the most important achievements in this study is the ambipolar characteristics of transistors. As we discussed above, most of solution processed SWNT FETs so far show only unipolar hole-conduction and the generally accepted views for the suppression of electron conduction include: 1) large Schottky barrier at nanotube-electrode interface impedes electron injection; 2) the $-\text{OH}$ groups on the surface of dielectric layer act as traps for electrons; 3) the absorption of oxygen or water molecules suppresses electron conduction. The injection barrier could be ruled out as a major factor because the Schottky barrier formed at the interface between Au electrode (work function: 4.9) and carbon nanotubes with diameter around 0.9 nm (Fermi level: 4.5 eV) [52] reaches as high as 1 eV, which is much larger than the one between Au and SWNTs with diameter larger than 1.1 nm [53]. It indicates that matching the work function of the metal electrode with the energy level of carbon nanotubes is not required for ambipolar operation. We can therefore conclude that the ambipolarity of SWNT transistor benefits from the surface treatment on dielectrics with APTES that reduced the density of $-\text{OH}$ group, also from the fact that the sample preparation was free of water.

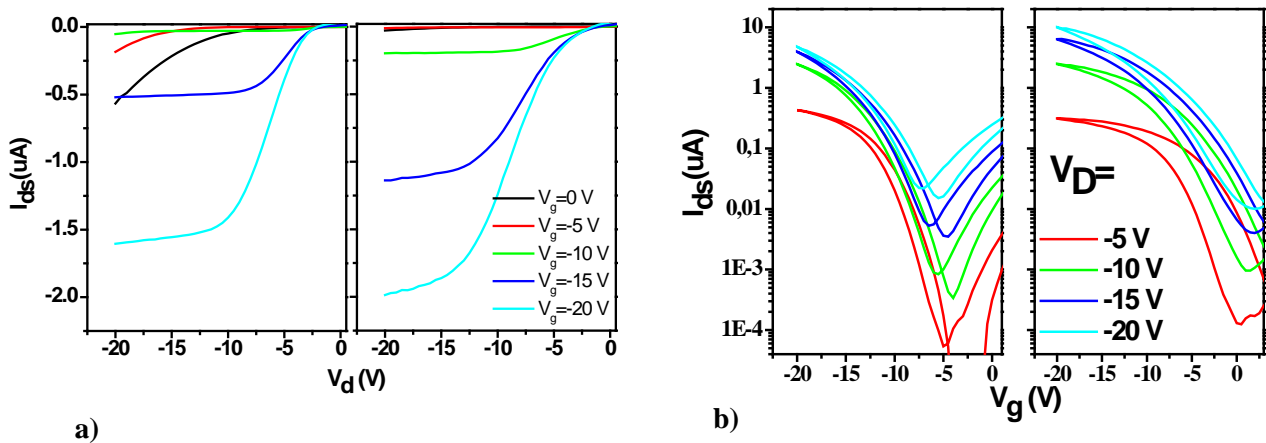


Figure 4. Ambient experiment. P-type output (a) and transfer (b) curves of device with 20 μm channel length before and after 1 day exposition in air atmosphere are shown.

In order to investigate the effects of ambience on the performance of SWNT devices, we exposed the devices to ambient environment ($\sim 70\%$ relative humidity at 20°C) for up to 24 hours and performed I-V measurements under the same conditions. We observed a general effect of ambient air on the device that induced an increase in hole transport as well as a decrease in electron conduction. In the Fig. 4a where left trend represents measurement made in the vacuum and the right curve represents measurements after 1 day exposure in the air. As could be seen from the plot that the hole current increased after exposition in air atmosphere the same behavior of the drain source current could be seen from the transfer characteristics Fig. 4b. So as consequence hole mobility increased from 7.5×10^{-3} to $1.2 \times 10^{-2} \text{ cm}^2/\text{V s}$ after 24 hour exposure and the threshold voltage V_{th} for p-channel showed positive shifts (-4 V to 4 V). As concerning of the n-channel transport, it degraded with exposure to air and no current was observed after 24 hours with gate bias up to 60 V . Such variations have also been observed in single or double-walled carbon nanotube FETs [54-55] and two possible mechanism have been proposed: 1) the work function of electrode increases with exposure in air, which results in an improved p type behavior; 2) Adsorbed water (H_2O) and/or oxygen (O_2) molecules electrochemically modify the electronic properties SWNTs, which leads to a suppression of electron conduction [56]. The positive shift of threshold voltage and the degradation of n type characteristics indicate an increased hole density in the active layer. We therefore conclude the second mechanism is the dominant factor that responsible for the suppression of electron conduction in SWNTs. These two assumption is in a good agreement with the previously proposed mechanism that also was mentioned in 3.2.1 section, that electrochemically mediated charge transfer process from SWNTs to the water and oxygen redox coupling take place.

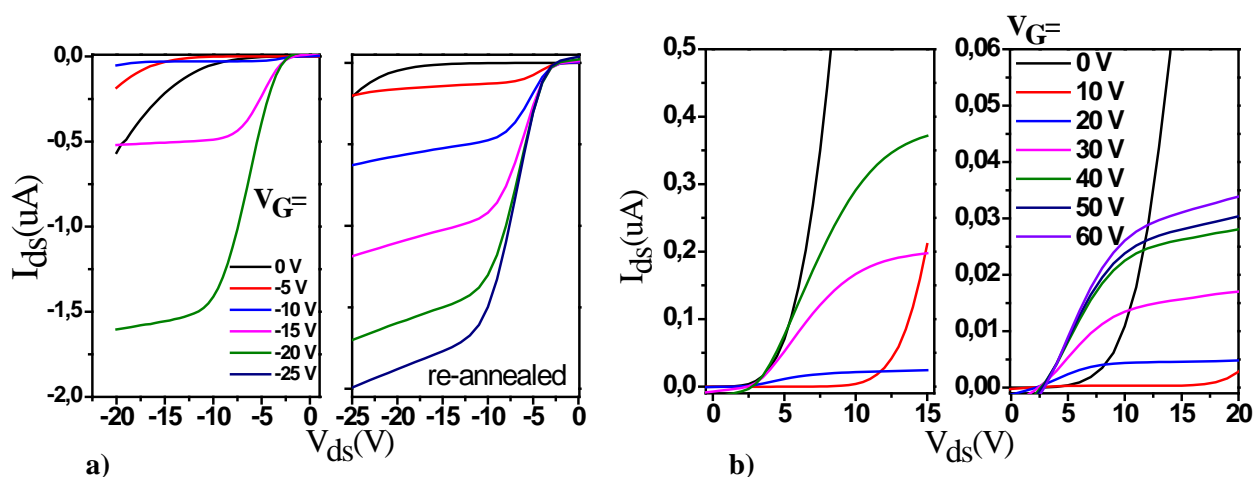


Figure 4.1. Re-annealing experiment. (a) p-channel output curves, left plot represents measurements in vacuum and right plot represents measurements after re-annealing procedure (b) n-channel output curves, left plot represents measurements in vacuum and right one after re-annealing. Channel device has length 20

For the further understanding of ambience-stability of am bipolar SWNT FETs we did re-measurements of I-V characteristics of the device that the was exposed again de in vacuum after vacuum annealing at 150 °C for 2 hours. (Fig.4.1)We observed a recovery of the starting performance in p-channel. The hole mobility and showed almost no change compare to the initial values $\mu_h \sim 8 \times 10^{-3} \text{ cm}^2 \text{ V}^{-1} \text{ s}^{-1}$ but threshold voltage for p-channel showed small positive shifts (-4 V to -2 V). In n-range, the electron mobility of the device re-annealed is lower than the starting value ($1.3 \times 10^{-3} \text{ cm}^2 \text{ V}^{-1} \text{ s}^{-1}$ compare to $3.1 \times 10^{-3} \text{ cm}^2 \text{ V}^{-1} \text{ s}^{-1}$) and the threshold voltage shifts towards positive direction (10 V to 30 V). The gate hysteresis of the FET after re-annealing in vacuum is also larger than starting device

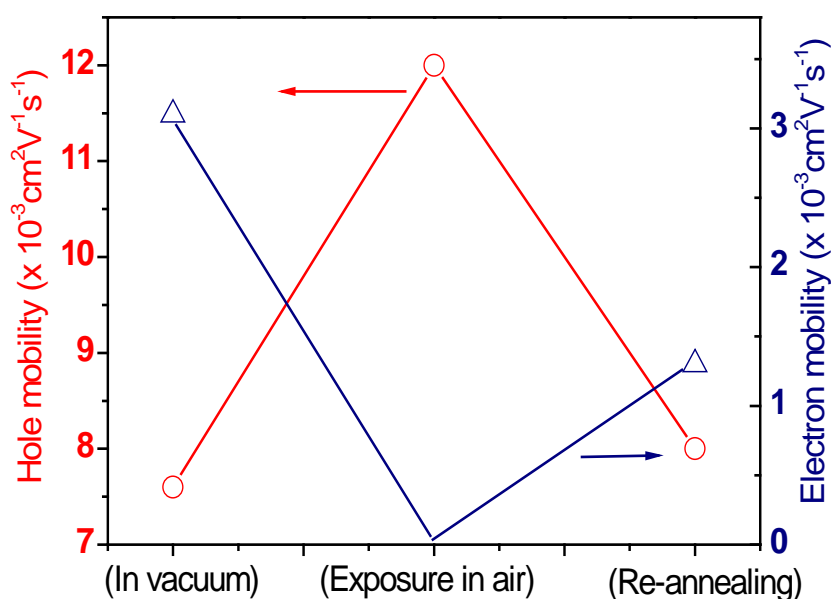


Figure 4.2. Variations of device mobility with exposure to air ambience. This graph summarizes the ambient effect on the mobility of ambipolar SWNT FETs.

The summary graph (Fig.4.2) shows clearly ambient effect. The mobility it is very sensitive to the ambient conditions. After 24 hours at the air exposition, n-type transport was completely suppressed and holes mobility increased on the contrary. When we did re-annealing procedure we almost recovered completely p-type transport, but we cannot restore fully the n- channel degradation after 24 hours exposition in the air

3.2.8. High-temperature annealing in air.

The effect of annealing in air on the electrical performance of SWNT devices was also investigated. Fresh devices without exposure in air were annealed in air at 400 °C for 2 hours and the electrical characteristics of the transistor (20 μm channel length) before and after annealing are shown in Figure 4.3. All ambipolar transistors converted into p type unipolar devices and some performance improvements were observed.

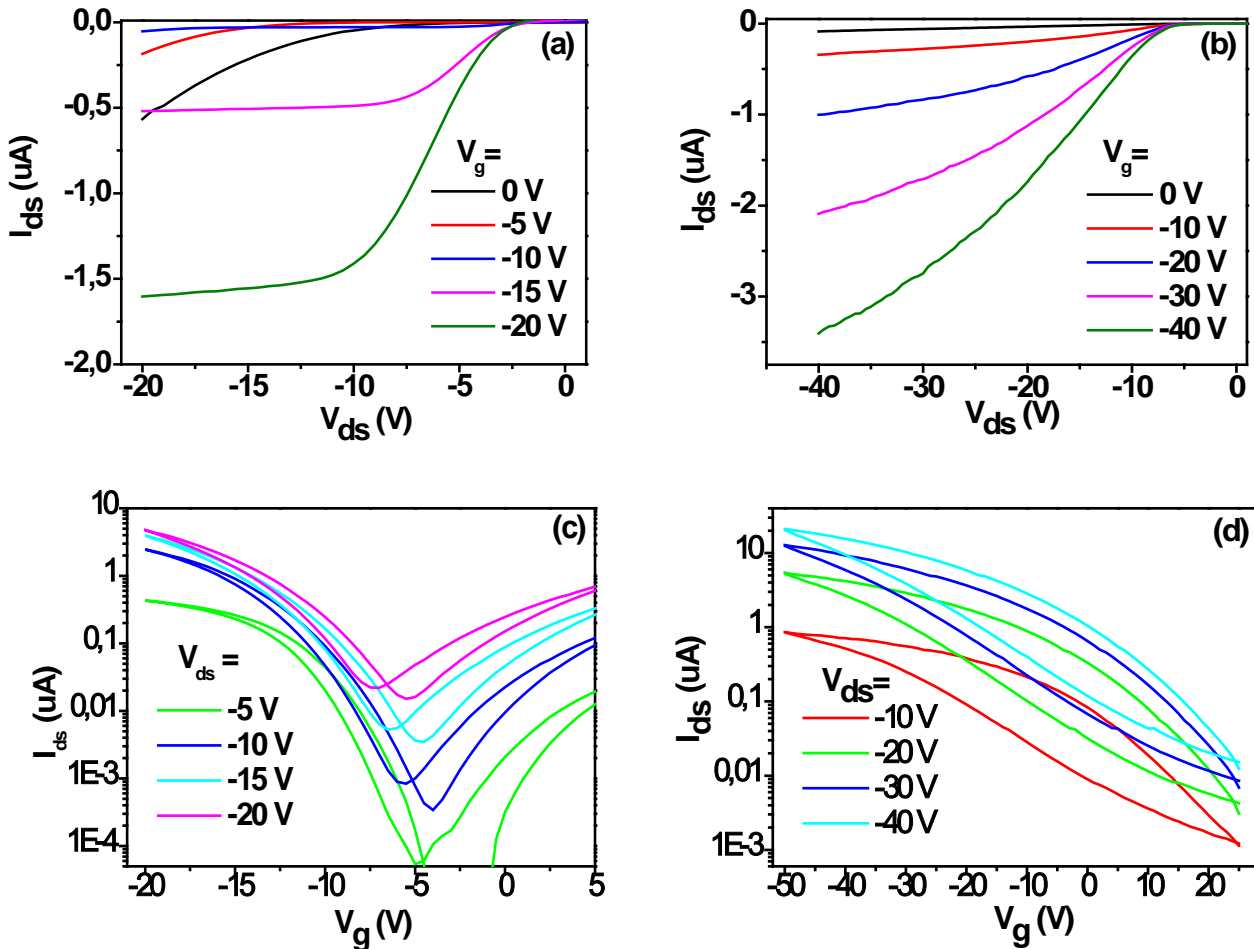


Figure 4.3. Output and transfer curves of the device with 20 μm channel length before (a), (c) and after annealing in air (b) (d).

The saturation regime in output curves in the device after annealing Fig. 4.3b is less pronounced than the fresh one Fig 4.3a. We could rationalize such variation by taking into account of the contribution of two resistances: the contact resistance (electrode/tube) and the channel resistance (tube/tube). In the case of fresh devices, the channel resistance is the major factor that determines carrier transport in SWNT transistors and can be modulated by gate bias. Saturation regime then could be observed in output characteristic measurements. After the removal of residual polymers that form tunneling barriers [57], both electrode/tube and tube/tube resistance were reduced. However, the parasitic contact resistance between the electrode and SWNTs remains and plays a more important role than that the channel

resistance. The device behaves analogues to a Schottky barrier transistor, in which switching occurs primarily by modulation of the contact resistance rather than the channel resistance. Transfer characteristics of the devices before and after air annealing are shown in Fig 4.3c and Fig 4.3d. The device after annealing in air shows a hysteresis in current as high as 190 nA (gate bias -10V), which is much larger than that in the starting device ~ 44 nA. It can be rationalized as due to the destructive effects on the self-assembled molecules with high temperature treatment. Also the influence from the residual impurity (e. g. destroyed polymer chains) should not be neglected.

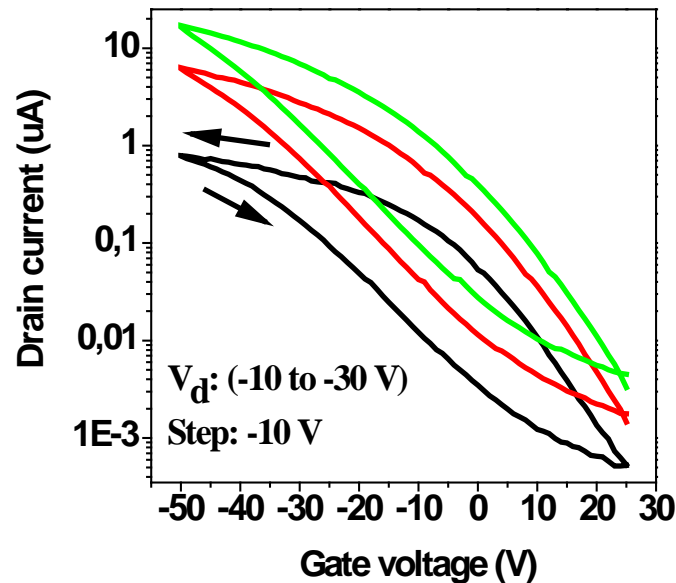


Figure. 4.4. Transfer curves of device with 20 μm channel length after annealing in air

Fig. 4.4 represent transfer curves of device with channel length 20 μm after annealing procedure in air. It is clear to see that the sweeps in all the devices show the hysteresis is advancing in nature instead of retarding. This is the typical sign of the surface traps in the dielectric layer which is commonly observed in SWNT transistors [58-59]. It implies the necessities of surface modification and water-free sample preparation for the ambipolar characteristics in SWNT transistors. Summary plot of device performances like mobility and on/off ratio versus channel length is shown below. It was calculated and plotted dependence mobility for Forward and Back sweep separately versus channel length of device. It is clear to see that the mobility for forward scan is lower (range $0,5-1 \times 10^{-2} \text{cm}^2 \text{V}^{-1} \text{s}^{-1}$) than for back sweep (range $1-3 \times 10^{-2} \text{cm}^2 \text{V}^{-1} \text{s}^{-1}$). It indicates the presence of carrier trapping on the surface on SWNTs, as we discussed in this work many times most likely that the silanol groups with oxygen and water are the main traps for electrons and also probably polymer residue may be trap for holes.

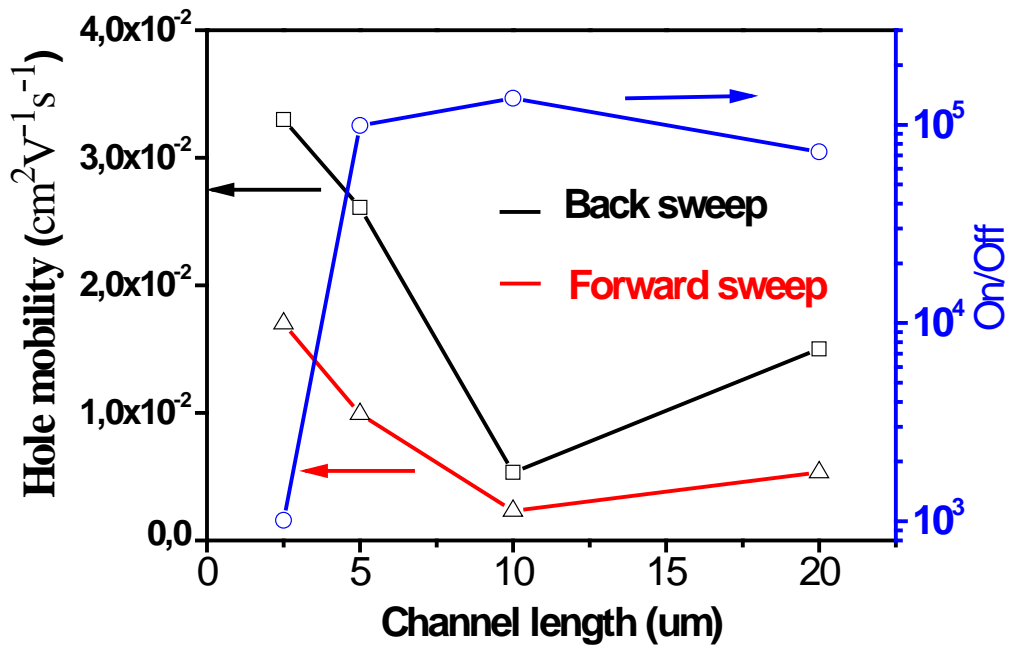


Figure. 4.5. summarize plot for the performances dependence (mobility and on/off ratio) of the device versus different channel length

Also as can be seen from Fig.4.5. after high temperature burning we observed On/off ratio increase comparing to the first measurements in vacuum. It could be explained in the simple way, because using high temperature annealing we burned out most of polymer and in this case decreased coupling capacitance between SWNT network and SiO₂ substrate also reduced metal-nanotube contact resistance and reduced tube-tube coupling resistance. It is important to mentioned that now On/Off ration reaches 10⁵ and if comparing with 95% semiconducting SWNTs FET out device has mobility bigger in one order of magnitude.

Chapter 4

Conclusion and future research

4.1 Conclusion

In this thesis we demonstrated the realization of ambipolar field effect transistor of both hole and electron transport by using high purity semiconducting single-walled carbon nanotube dispersion. We firstly dispersed SWNT powders in organic solution and after using several method of sorting, that only consists of sonication and ultracentrifugation procedure, we developed a scalable method for preparation of high purity semiconducting SWNT suspension. After this step, dispersion could be deposited on the substrate with pre-patterned electrodes by spincoating or dropcasting technique and in this way SWNT FET could be fabricated. However the electron transport in another words n-type character is strongly suppressed or completely absent in the device fabricated following protocol in almost all citations, our method to fabrication of ambipolar SWNT network FET is some kind unique. Also it is necessary to mention that our process is much less time-consuming with the aid of ultracentrifugation. In current project was fabricated two types of SWNT FETs. First type of devices was fabricated using commercial available aqueous surfactant solution which contains 95% of semiconducting species. For device fabrication was used several spincoating programs. Unipolar p-type SWNT FETs with low on/off ration near 20 were obtained as was expected before. Second types of devices was built using our “home made” suspension with higher purity of semiconducting species by dropcasting procedure. Two most important points were stressed for evaluation of SWNT FETs: firstly the coverage of SWNTs in the channel region and secondly concentration of metallic tubes in SWNT network. After comparing two types of devices which each other one can say for sure that device which was prepared by commercial available suspension (95%) shows a little bit higher mobility that the prepared with high purity semiconducting SWNT(99%) by taking advantage of certain amount of metallic species in channel. But comparing of the on/off ratio parameter shows that on/off ration of the “devices made by “home made” suspension in three order magnitude higher than of the device which was built using commercial available solution also this result is in good agreement with optical measurement of “home made” suspensions which proves that our home made suspension has high purity of semiconducting species. One of the most important results of our study is the fact that we are able to get ambipolar transistor. Because, as we told before most of solution processed SWNT FETs so far show only unipolar hole-conduction behavior. Ambipolar operation has been observed in solution processed SWNT transistors and device mobility was in the range 10^{-2} - 10^{-3} $\text{cm}^2/\text{V s}$ in both p and n channels. In terms of study traps in ambipolar SWNT network FETs was study effects of ambience on the performance of SWNT devices. We demonstrate extrinsic effects on the electrical characteristics of SWNT FETs. Hole mobility increased with exposure in air and the threshold voltage of p-channel showed positive shifts. On the contrary, n-channel characteristics degraded with air exposure and completely suppressed after 24 hours. The effect of high

temperature air annealing (400° C) on device performance is also shown, this procedure converted ambipolar FETs into p type only devices with mobility in range of $1 \times 10^{-2} \text{ cm}^2\text{V}^{-1} \text{ s}^{-1}$ and on/off ratio higher than 10^5 and led to a larger gate hysteresis.

4.2 Future research

As was shown in many theoretical and practical works, PFO has the affinity to interact with semiconducting nanotube species and this fact could open the very promising path to a commercially feasible carbon nanotubes creation process is real, however a lot of issues need to be addressed. First of all PFO should be used in SWNT powder which has a narrow chiral vector band distribution with a high concentration of (8,6) and (8,7) tubes. Necessary to say that the mixture of SWNTs, PFO and toluene with a ratio of 1 mg:3 mg:10 ml showed quite good results so far. So this leads to the question if it is possible to make a better device performance if using lower amount PFO concentration. After ultracentrifuge procedure the large bundles sank to the bottom, but of course some small bundles which contain metallic species are still in suspension. Concerning the fact that if we increase g-force even more we are able to get semiconducting suspension with purity even higher than 98-99%. Also the time of ultracentrifuge procedure is also important as was seen from experiment after 6 hours of ultracentrifuge procedure toluene starts to melt polyallomer tube which is a limit for us. Second crucial point is that performance of SWNT FET depends from SWNT coverage of channel. In our project we got SWNT network FET with coverage less than 1% with decent ambipolar performances, but it is no doubt that if we increase the coverage of the channel, the SWNT FET performances like mobility and on/off ratio have to increase. Concerning the fact that our devices are very sensitive to ambient conditions is a good idea to burn them in an atmosphere different from air, such as Nitrogen or Argon atmosphere and to study the influence of this procedure. So it is possible to take more experiments with different ambient conditions to have a deeper understanding of the mechanism of surface traps in single carbon nanotubes. And it seems that these series of experiments are very promising. Also it is very interesting from a practical interest to incorporate our suspension into different practical applications. For instance it is a very promising idea to try to use our suspension with high semiconducting species purity in other types of devices, like photodetectors and solar cells.

Acknowledgements

I would like to thank Prof.Dr.Maria Antonietta Loi for being a supervisor of my master project and also for her help. I am also very grateful to my daily supervisor Ph.D student Jia Gao for his help and instructions on the usage of the lab equipment, for all suggestions and many very useful discussions and being kind to give answers for all my questions. Jan and Frans I appreciate your technical support. It has been a nice time working with the Physics of Organic Semiconductors group. Thanks to all group members who are open to each other for a really friendly atmosphere in the group. Thanks to Zernike Institute for Advanced Materials for giving me a unique opportunity to be a student of the Top Master in Nanoscience Program during the last two years.

Especially I would like to thank to Prof.Dr.Maria Antonietta Loi, Dr.Koos Mars and my mentor Prof. Casper Van der Wall for that they gave me chance to finish Top Master Programme in Nanoscience and their huge help for me, when I needed it.

Bibliography

- [1]. S. Iijima, "Helical Microtubules of Graphitic Carbon," *Nature*, vol. 354, pp. 56-58, 1991.
- [2]. R. H. Baughman, A. A. Zakhidov, and W. A. de Heer, "Carbon nanotubes – the route toward applications," *Science*, vol. 297, pp. 787-792, 2002.
- [3]. R. Martel, T. Schmidt, H. R. Shea, T. Hertel, and P. Avouris, "Single- and multiwall carbon nanotube field-effect transistors," *Applied Physics Letters*, vol. 73, pp. 2447-2449, 1998.].
- [4]. P. Avouris, J. Appenzeller, R. Martel, and S. J. Wind, "Carbon nanotube electronics," *Proceedings of the Ieee*, vol. 91, pp. 1772-1784, 2003.
- [5]. P. L. McEuen, M. S. Fuhrer, and H. K. Park, "Single-walled carbon nanotube electronics," *Ieee Transactions on Nanotechnology*, vol. 1, pp. 78-85, 2002.
- [6]. Ebbesen, T. W. & Ajayan, P. M. Large-scale synthesis of carbon nanotubes. *Nature* 358, 220–222, 1992.
- [7]. Guo, T., Nikolaev, P., Thess, A., Colbert, D. T. & Smalley, R. E. Catalytic growth of single-walled nanotubes by laser vaporization. *Chem. Phys. Lett.* 243, 49–54, 1995.
- [8]. Endo, M. *et al.* The production and structure of pyrolytic carbon nanotubes. *J. Phys. Chem. Solids* **54**, 1841–1848, 1993.
- [9]. Krupke, R. & Hennrich, F. Separation techniques for carbon nanotubes. *Adv. Engineer. Mat.* **7**, 111–116 (2005). Banerjee, S., Hemraj-Benny, T. & Wong, S. S. Routes towards separating metallic and semiconducting nanotubes. *J. Nanosci. Nanotechnol.* **5**, 841–855, (2005).
- [10]. Haddon, R. C., Sippel, J., Rinzler, A. G. & Papadimitrakopoulos, F. Purification and separation of carbon nanotubes. *Mater. Res. Bull.* **29**, 252–259 (2004).
- [11]. Michael J. O'Connell, Band Gap Fluorescence from Individual Single-Walled Carbon Nanotubes, *Science*, Vol. 297, pp. 593-596, 2002.
- [12]. M. F. Islam et al., High Weight Fraction Surfactant Solubilization of Single-Wall Carbon Nanotubes in Water, *Nano Letters*, pp 269–273, 2003
- [13]. Harald Hope, et. al. Nanoscale Morphology of Conjugated Polymer/Fullerene-Based-Bulk- Heterojunction Solar Cells, *Adv. Funct. Mater.* **14**, 1005-1011, 2004.
- [14]. Mark C. Hersam, *Nature Nanotechnology* **3**, 387 - 394 (2008).
- [15]. Robin J. Nicholas et. al., Polymer Structure and Solvent Effects on the Selective Dispersion of Single-Walled Carbon Nanotubes, *J. Am. Chem. Soc.*, **130** (11), pp. 3543–3553, 2008.
- [16]. J. Gao and M. A. Loi, Photophysics of polymer-wrapped single-walled carbon nanotubes *Eur. Phys. J. B* **75** 2 (2010) 121-126.

- [17]. Gao J, Kwak M, Wildeman J, Herrmann A, Loi MA, Effectiveness of sorting single-walled carbon nanotubes by diameter using polyfluorene derivatives, *Carbon* 2011, 49, 333-338.
- [18]. Dai,H, et. al. Carbon nanotubes: opportunities and challenges. *Surface Science*, 500, 218-241.
- [19]. J. Appenzeller, J. Knoch, V. Derycke, R. Martel, S. Wind, and P. Avouris, "Fieldmodulated carrier transport in carbon nanotube transistors," *Physical Review Letters*, vol. 89, pp. 126801.1-126801.4, 2002.
- [20]. S. Heinze, J. Tersoff, R. Martel, V. Derycke, J. Appenzeller, and P. Avouris, "Carbon nanotubes as Schottky barrier transistors," *Physical Review Letters*, vol.89, pp. 106801.1-106801.4, 2002.
- [21]. J. Guo, S. Datta, and M. Lundstrom, "A numerical study of scaling issues for Schottky-Barrier carbon nanotube transistors," *Ieee Transactions on Electron Devices*, vol. 51, pp. 172-177, 2004.
- [22]. M. Radosavljevic, S. Heinze, J. Tersoff, and P. Avouris, "Drain voltage scaling in carbon nanotube transistors," *Applied Physics Letters*, vol. 83, pp. 2435-2437, 2003.
- [23]. S. J. Wind, J. Appenzeller, R. Martel, V. Derycke, and P. Avouris, "Fabrication and electrical characterization of top gate single-wall carbon nanotube field-effect transistors," *Journal of Vacuum Science & Technology B*, vol. 20, pp. 2798-2801.
- [24]. Shunjiro Fujii et al, Performance Enhancement of Thin-Film Transistors by Using High-Purity Semiconducting Single-Wall Carbon Nanotubes, *Applied Physics Express* 2 (2009) 071601.
- [25]. Takeshi Tanaka et al, Simple and Scalable Gel-Based Separation of Metallic and Semiconducting Carbon Nanotubes, *Nano Lett.*, pp 1497–1500, 9 (4) 2009.
- [26]. Chun Wei Lee et al., Solution-Processable Carbon Nanotubes for Semiconducting Thin-Film Transistor Devices, *Adv. Mater.*, 22, 1278–1282, 2010.
- [27]. S. Heinze, J. Tersoff, R. Martel, V. Derycke, J. Appenzeller, and P. Avouris, "Carbon nanotubes as Schottky barrier transistors," *Physical Review Letters*, vol.89, pp. 106801.1-106801.4, 2002.
- [28]. Carla M. Aguirre, Pierre L. Levesque, Matthieu Paillet, François Lapointe, Benoit C. St-Antoine, Patrick Desjardins, and Richard Martel, The Role of the Oxygen/Water Redox Couple in Suppressing Electron Conduction in Field-Effect Transistors, *Adv. Mater.*, 2009, 21, 3087–3091.
- [29]. Tans, S. J.; Verschueren, A. R. M.; Dekker, C. *Nature* 1998, 393,49.

- [30]. Martel, R.; Derycke, V.; Lavoie, C.; Appenzeller, J.; Chan, K. K.; Tersoff, J.; Avouris, P. *Phys. Rev. Lett.* 2001, 87.
- [31]. Misewich, J. A.; Martel, R.; Avouris, P.; Tsang, J. C.; Heinze, S.; Tersoff, J. *Science* 2003, 300, 783.
- [32]. Freitag, M., Chen, J., Tersoff, J., Tsang, J. C., Fu, Q., Liu, J., Avouris, P. *Phys. Rev. Lett.* 2004, 93, 076803
- [33]. Joon Sung Lee et al. Origin of Gate Hysteresis in Carbon Nanotube Field-Effect Transistors, *Journal of physical chemistry C*, 111, 12504-12507, 2007.
- [34]. Minni Qu et al., Charge-Injection-Induced Time Decay in Carbon Nanotube Network-Based FETs, *IEEE ELECTRON DEVICE LETTERS*, vol. 31, no.10, 2010.
- [35]. Arnaud Robert-Peillard and Slava V. Rotkin, Modeling Hysteresis Phenomena in Nanotube Field-Effect Transistors, *IEEE TRANSACTIONS ON NANOTECHNOLOGY*, vol. 4, no. 2, 2005
- [36]. Manfred M. Kappes et al. Near Monochiral Single-Walled Carbon Nanotube Dispersions in Organic Solvents, *J. Phys. Chem. C*, 2009, 113 (33), pp 14628–14632
- [37]. N. Izard, et. al. Semiconductor-enriched single wall carbon nanotube networks applied to field effect transistors, *Appl. Phys. Lett.* 92, 243112 (2008).
- [38]. A. Vijayaraghavan, F. Hennrich, N. Stürzl, M. Engel, M. Ganzhorn, M. Oron-Carl, C.W. Marquardt, S. Dehm, S. Lebdkin, M.M. Kappes, R. Krupke, Toward Single-Chirality Carbon Nanotube Device Arrays *ACS Nano* 4 (2010) 2748–2754.
- [39]. Wei Zhi Wang, et. al. Degradable Conjugated Polymers: Synthesis and Applications in Enrichment of Semiconducting Single-Walled Carbon Nanotubes, *AFM* 21 1643, 2011.
- [40]. Xianlong Wei, et. al. Phonon-Assisted Electron Emission from Individual Carbon Nanotubes, *Nano letter* 11, 455, 2011.
- [41]. S. Heinze, et. al. Carbon Nanotubes as Schottky Barrier Transistors, *PRL* 89, 106801 (2002).
- [42]. Richard Martel, et. al. The Role of the Oxygen/Water Redox Couple in Suppressing Electron Conduction in Field-Effect Transistors, *Adv Mater* Vol 21, pp.3087-3091, 2009.
- [43]. Phaedon Avouris et. al. Thin Film Nanotube Transistors Based on Self-Assembled, Aligned, Semiconducting Carbon Nanotube Arrays *ACS Nano*, 2008, 2 (12), pp 2445–2452
- [44]. Chuan Wang, et. al. Wafer-Scale Fabrication of Separated Carbon Nanotube Thin-Film Transistors for Display Applications, *Nano Lett.*, 2009, 9 (12), pp 4285–4291]

- [45]. E. S. Snow, et. al. High-mobility carbon-nanotube thin-film transistors on a polymeric substrate , *Appl. Phys. Lett.* 86, 033105 (2005).
- [46]. Qing Cao, et. al. Gate capacitance coupling of singled-walled carbon nanotube thin-film transistors, *Appl. Phys. Lett.* **90**, 023516, 2007 .
- [47]. Slava V. Rotkin , John A. Rogers, High-performance electronics using dense, perfectly aligned arrays of single-walled carbon nanotubes, *Nature Nanotechnology* 2, 230 - 236 (2007).
- [48]. Chuan Wang, et.al. Macroelectronic integrated circuits using high-performance separated carbon nanotube thin-film transistors, *ACS Nano*, Vol. 4, No. 12, 7123-7132 (2010).
- [49]. Haruya Okimoto, et. al. Tunable Carbon Nanotube Thin-Film Transistors Produced Exclusively via Inkjet Printing, *Adv mat* 22, 3981, 2010.
- [50]. R. Ruiz, et. al. Thickness Dependence of Mobility in Pentacene Thin-Film Transistors *Advanced Materials*, vol. 17, pp 1795-1798, 2005.
- [51]. Jia Gao et. al. Controlling of the surface energy of the gate dielectric in organic field-effect transistors by polymer blend, *Appl. Phys. Lett.* **94**, 093302 (2009)
- [52]. M. Radosavljević, Nonvolatile Molecular Memory Elements Based on Ambipolar Nanotube Field Effect Transistors, *Nano Letters*, 2002, 2 (7), pp 761–764.
- [53]. Ali Javey, Moonsub Shim, and Hongjie Dai ,Electrical properties and devices of large-diameter single-walled carbon nanotubes , *Appl. Phys. Lett.* 80, 1064 (2002)
- [54]. Donghun Kang, et.al. Adsorption-induced conversion of the carbon nanotube field effect transistor from ambipolar to unipolar behavior , *Appl. Phys. Lett.* 86, 093105 (2005).
- [55]. V. Derycke, R. Martel, and Ph. Avouris,. *Appl. Phys. Lett.* 80, 2773, 2002.
- [56]. Carla M. Aguirre, et. al. The Role of the Oxygen/Water Redox Couple in Suppressing Electron Conduction in Field-Effect Transistors, *Adv Mater* 21, 3087, 2009.
- [57]. Aravind Vijayaraghavan, et.al. Ultra-Large-Scale Directed Assembly of Single-Walled Carbon Nanotube Devices, *Nano Lett.*, 7pp 1556–1560, 2007,
- [58]. Woong Kim, et.al. Hysteresis Caused by Water Molecules in Carbon Nanotube Field-Effect Transistors, *Nano Letters*, pp 193–198, 2003.
- [59]. Chun Wei Lee, et. al. Solution-Processable Carbon Nanotubes for Semiconducting Thin-Film Transistor Devices, *Adv Mater*, 22, 1278, 2010
- [60]. Chuan Wang, et.al. Wafer-Scale Fabrication of Separated Carbon Nanotube Thin-Film Transistors for Display Applications, *Nano Lett.*, 9 (12), pp 4285–4291, 2009,

Appendix A: Device based on commercial available suspension

Channel length 20 μm

Programm №	$\mu_p \left(\frac{\text{cm}^2}{\text{V}\cdot\text{s}}\right)$	V_{th}	$\frac{on}{off}$ ration	On current
1 DropCast	$2,7 \times 10^{-3}$	10 V	2	20 μA
2 1 step -300 rpm(10 sec) 2 nd step -500 rpm(60 sec)	$1,33 \times 10^{-2}$	12 V	2	1mA
3 1 step -660 rpm(10 sec) 2nd step -1500 rpm (60 sec)	$1,79 \times 10^{-2}$	-2 V	13	15 μA
4(Ambipolar) 1 step -1000 rpm(10 sec) 2nd step -1500 rpm (60 sec)	$2,7 \times 10^{-4}$	-6V	30	0,25 μA
5 1 step -600 rpm(10 sec) 2nd step -2000 rpm (60 sec)	$4,325 \times 10^{-2}$	7 V	4	30 μA
6 1 step -1000 rpm(10 sec) 2nd step -3000 rpm (60 sec)	Huge leakage			
7 1 step -1500 rpm(10 sec) 2nd step -3000 rpm (60 sec)	Huge leakage			

Fig 1. Appendix A. Summary table of all spincoating programs for device with channel length 20 μm

Channel length 10 μm

Programm №	$\mu_p \left(\frac{\text{cm}^2}{\text{V}\cdot\text{s}}\right)$	V_{th}	$\frac{on}{off}$ ration	On current
1 Dropcast	Low current 5×10^{-6}	10	1,5	0,05 μA
2 1 step -300 rpm(10 sec) 2 nd step -500 rpm(60 sec)	1×10^{-2}	8 V	2	100 μA
3 1 step -660 rpm(10 sec) 2nd step -1500 rpm (60 sec)	1×10^{-2}	0 V	1,5	10 μA
4 1 step -1000 rpm(10 sec) 2nd step -1500 rpm (60 sec)	$2,7 \times 10^{-3}$	-3 V	26	1 μA
5 1 step -600 rpm(10 sec) 2nd step -2000 rpm (60 sec)	$2,7 \times 10^{-2}$	7 V	3	50 μA
6 1 step -1000 rpm(10 sec) 2nd step -3000 rpm (60 sec)	Huge leakage			
7 1 step -1500 rpm(10 sec) 2nd step -3000 rpm (60 sec)	Huge leakage			

Fig 2.Apendix A. Summary table of all spincoating programs for device with channel length 20 μm

Channel length 5 μm

Programm №	$\mu_p \left(\frac{\text{cm}^2}{\text{V}\cdot\text{s}}\right)$	V_{th}	$\frac{on}{off}$ ration	On current
1 Dropcast	Low curren $3,3 \times 10^{-6}$	More 10	1	0,01ua
2 1 step -300 rpm(10 sec) 2 nd step -500 rpm(60 sec)	10^{-3}	More than 10	2	200 uA
3 1 step -660 rpm(10 sec) 2nd step -1500 rpm (60 sec)	$1,65 \times 10^{-1}$	More than 10	1.5	1mA
4 1 step -1000 rpm(10 sec) 2nd step -1500 rpm (60 sec)	$8,8 \times 10^{-5}$	0 V	12	2uA
5 1 step -600 rpm(10 sec) 2nd step -2000 rpm (60 sec)	$1,1 \times 10^{-2}$	10 V	2	100uA
6 1 step -1000 rpm(10 sec) 2nd step -3000 rpm (60 sec)	Huge leakage			
7 1 step -1500 rpm(10 sec) 2nd step -3000 rpm (60 sec)	Huge leakage			

Fig 3.Apendix A. Summary table of all spincoating programs for device with channel length 20 μm